MACQUARIE
University

Geophysical signatures of small-scale base metal occurrences in south eastern NSW

Harrison W. W. Jones
Master of Research Thesis

Department of Earth and Planetary Sciences in the Faculty of Science and Engineering, Macquarie University, North Ryde, Australia.

Coursework study – July 2015 – May 2016 (~12 months)
Thesis research – June 2016 – April 2017 (~10 months)
Thesis submission – 24/04/2017
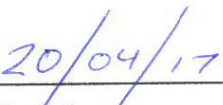

Above Photo: Gurubang Deposit

CCFS

Australian Society of
Exploration Geophysicists

Statement of Originality

All the work submitted in this thesis is the original work of the author except were otherwise acknowledged. No part of this thesis has been previously submitted to any other university or institution.

Signed – *Harrison Jones*

20/04/17

Dated

ACKNOWLEDGMENTS

To my Uncle Stan, you were the reason I became interested in the geosciences and to show my appreciation this thesis is dedicated to you.

TABLE OF CONTENTS

CHAPTER 6: CONCLUSION

REFERENCES

Geophysical signatures of small-scale base metal occurrences in south eastern NSW

ABSTRACT

Ground-based, time-domain electromagnetic, magnetic and gravity datasets were obtained for the southern Gurubang and Rosebank VHMS deposits located approximately 15 km east of Cooma, NSW. The deposits are hosted in a mid-late Silurian sequence of rock composed of shallow marine sediments and felsic volcanic rocks. The aim of this research was to ascertain the usefulness of high-resolution geophysical techniques in targeting and evaluating small-scale polymetallic massive sulphide deposits, and to investigate how the detailed geophysics relates to the overall geological framework of the prospect areas. The acquired data was analysed using a forward modelling approach. Due to both deposits containing high concentration of conductive minerals, a coincident loop time-domain electromagnetic 2D survey effectively delineated the sulphide mineralisation and was useful in interpreting and adapting deposit parameters such as the azimuth, dip and strike length. Based on the physical nature of the target deposits, it was determined that high-resolution magnetic and gravity surveys would not be effective methods in directly delineating these smaller-scaled (10's of m's) mineral deposits. However, magnetics and gravity did prove effective in depicting the surrounding geology, including potential volcanic intrusions and basement lithologies and structures.

Geophysical signatures of small-scale base metal occurrences in south eastern NSW

CHAPTER 1

THE GEOLOGY OF BASE METAL MINERALISATION

IN SOUTH EASTERN NSW

1.1 INTRODUCTION

Palaeozoic polymetallic volcanic-hosted massive sulphide (VHMS) deposits of south eastern New South Wales, have been a major source of Cu ± Au (e.g. Mt Morgan and Captains Flat) and a significant source of Pb – Zn – Ag (e.g. Woodlawn and Thalanga) over the last one hundred years of mining. Prior to the 1960s, all VHMS discoveries in Australia were based on outcropping gossans and mineralisation. However, more modern exploration commonly incorporates a multidisciplinary approach, using a combination of geological mapping to define volcanic facies, accompanied by geophysics and geochemistry to define drill targets (Gemmell, Large and Zaw, 1998).

In more recent times, geophysics has become an important tool in base metal exploration as companies turn their efforts towards buried and hidden deposits. Magnetic, gravity and electromagnetic methods have proven to be useful in VHMS detection. However, they are typically applied in large-scale prospecting (10's of km's) and may miss smaller, potentially profitable, deposits. VHMS deposits are considered relatively small-scale exploration targets (Gibson et. al., 2004).

There are several ways to characterise a small-scale mineral deposit. Typically, mineral deposits that are of limited spatial extent, discontinuous in nature with narrow widths and are found at shallow depths, qualify as small-scale. Shrivastava and Shrivastav (2015), states that small-scale deposits are often found as erratic and inconsistent in nature and are deposited as lenses, veins, pockets and cavities. These deposits are too small to be worked by large-scale mining. In this context, it is important to know the limitations of the geophysical methods and data when targeting such small-scale deposits. Also, a greater understanding of the optimum data resolution is needed for the range of geophysical methods.

1.2 RESEARCH OBJECTIVES

The aims of this project are to:

1. Ascertain the usefulness of high-resolution ground-based geophysics in the direct search and delineation of small-scale base metal deposits, and;
2. Investigate how the detailed geophysics relates to the geology of the designated project areas at a local and prospect scale.

With these aims defined, the following chapters will describe a geophysical investigation of the subsurface structure and base metal mineralisation of two small-scale VHMS deposits in south eastern NSW: the southern Gurubang, and Rosebank deposits. Whilst previous mineral exploration programs originally identified the two mineralised areas, the geophysical properties of these small-scale deposits have never been completely evaluated.

To evaluate the deposits, geological models were developed based on newly acquired geophysical data, in conjunction with prior geological interpretations and cores samples obtained across the two study localities. The forward modelling process was user controlled, in that the magnetic susceptibility, density and conductivity were manually modified until a reasonable fit was obtained between the measured and modelled data. Models were constructed to simulate the southern Gurubang $Pb - Zn \pm Cu$ deposit, and the Rosebank $Zn \pm Au$ deposit.

In successfully modelling the acquired dataset for each deposit location, one can then ascertain the effectiveness of the high-resolution methods in directly targeting the small-scale deposits (Airo, 2015). It will also provide further insight into the framework of the host geology. It is theorised that the electromagnetic method will probably be the most effective technique for directly identifying the mineralised VHMS horizons, due to the concentration of conductive minerals within each deposit as described in Castle, (1976) and Argaud, (1976). The high-resolution magnetic method should also provide useful information about the structure and geometry of the orebodies (Gunn and Dentith, 1997). High-resolution gravity surveys are uncommon in small-scale mineral exploration and may provide a new approach to targeting smaller deposits. As for examining the geological framework of the two deposit localities, the magnetic and gravity methods will probably be the most effective of the ground-based methods (Dentith and Mudge, 2014).

1.3 RESEARCH OUTCOMES

Desired outcomes of this research project are the following:

- A better understanding of the usefulness of ground-based geophysical methods in the direct search and delineation of small-scale base metal deposits;
- A better understanding of the resolution required to directly target and delineate small-scale base metal deposits for the range of geophysical methods;
- A better understanding of the characteristics of small-scale base metal deposits in south eastern NSW and how they are related to the geology at a local and prospect scale, and;
- A better understanding of the overall geological framework of the project areas at a local and prospect scale.

1.4 BACKGROUND GEOLOGY

The Lachlan Fold Belt in south eastern NSW

The Lachlan Fold Belt, or Lachlan Orogen, occupies majority of the central area of the north-south trending, Neoproterozoic to Mesozoic Tasmanides along Australia's eastern margin. The Lachlan Fold Belt is part of a Palaeozoic orogenic system that formed via massive telescoping and strike-slip translation within a continental margin sediment prism, along the former eastern margin of Gondwana (Gray, 1997). It is composed primarily of deformed deep-marine sedimentary rocks (quartz-rich turbidites), cherts, mafic volcanic rocks of Cambrian to Devonian age (520 Ma – 350 Ma), and younger cover sequences. Structurally, the Lachlan Fold Belt consists of a sequence of upright chevron folds, ranging from open to tight, as well as numerous steep crustal faults (Foster and Gray, 2000).
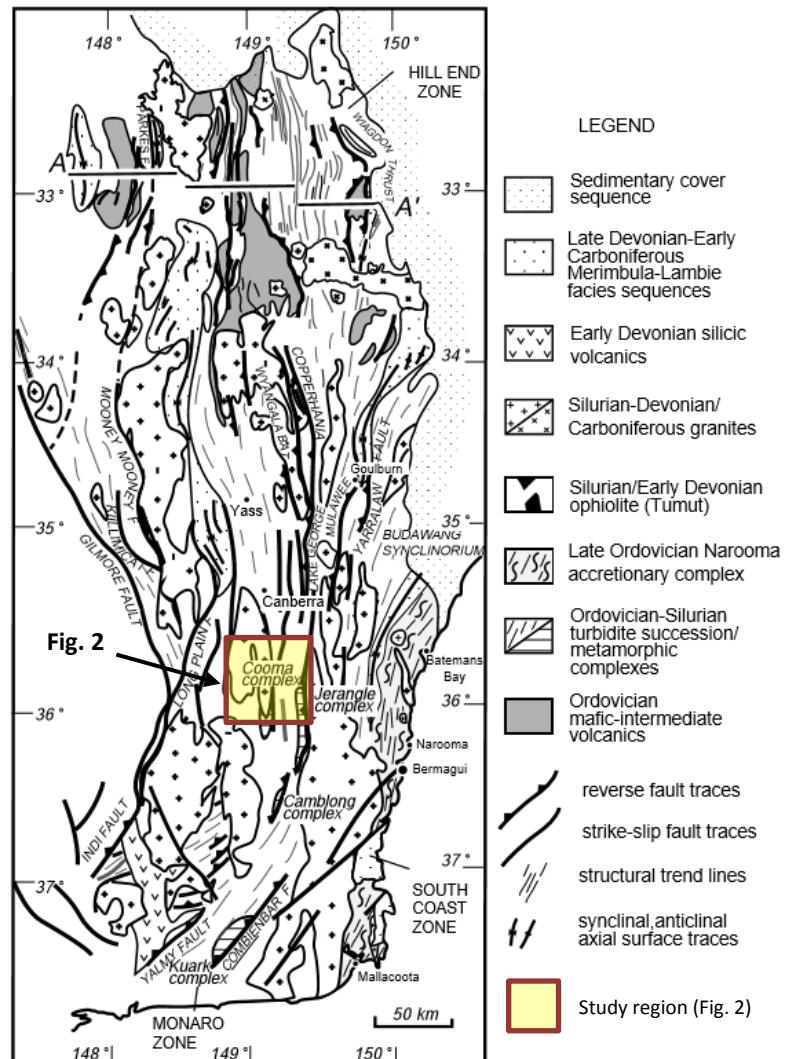
(Figure 1. Structural trend map and profile of the eastern Lachlan Orogen. Geological units and related major faults are shown (Foster and Gray, 2000). Project region is shown in Figure 2.)

The Lachlan Fold Belt is divided into three provinces; the west, central and east. Each province has different rock types, metamorphic grade, structural history and geological evolution. The east Lachlan province consists of mafic volcanic and volcaniclastic rocks, as well as carbonates, quartz-rich turbidites and extensive black shale situated in the eastern most area. The region is characterised by numerous open folded anticlinorial and synclinorial zones, which are bounded by both east and west dipping reverse faults (Foster and Gray, 2000).
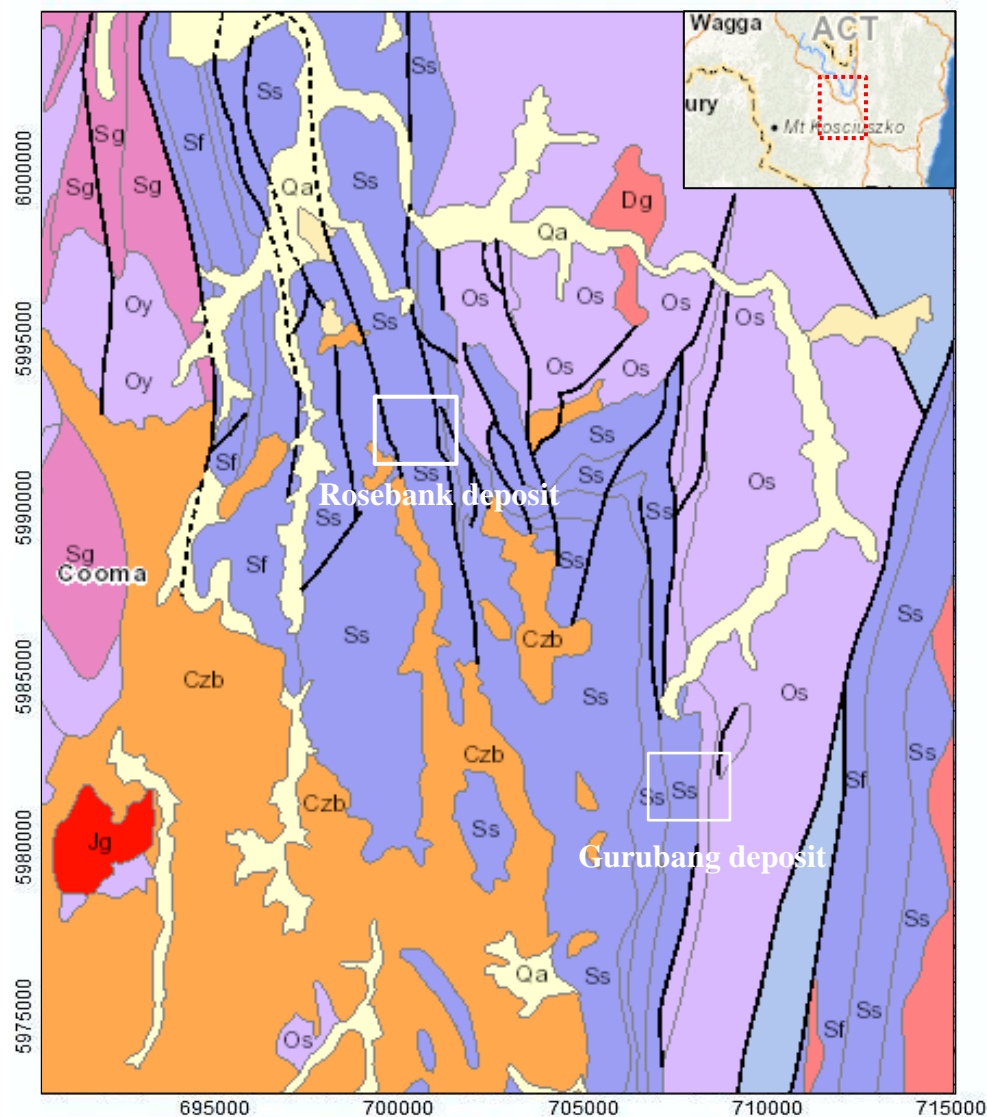
Cambrian Sediments

EOy	*Jerangle Metamorphic Complex*
	- metasediments

Ordovician Sediments

Os	*Bendoc Group*
	- siltstones, shales, sandstones
Oy	*Cooma Metamorphic Complex*
	- metasediments

Silurian Sediments/Volcanics/Intrusives

Ss, Sf	*Bredbo Group* **(Fig. 3)**
	- shallow marine sediments, I-type volcanics
Sg	*Silurian Granite*
	- I-type intrusive

Devonian Intrusives

Dg	*Devonian Granite*
	- I-type intrusive

Jurassic Intrusives

Jg	*Jurassic Granite*
	- I-type intrusive

Canozoic/Quaternary Sediments and Volcanics

Czb	*Cainozoic Sediments and Volcanics*
	- Alluvium and basalt
Qa	- Quaternary alluvial sediments

Major faults, accurate

Major faults, inferred

TN 0

Scale 1 : 120000
One centimetre is to 1200 metres

0m   2000m 4000m 6000m 8000m

(**Figure 2. Regional geological interpretation map of the Cooma region in the east Lachlan province. Image sourced from the Geology and Geophysics database from Geoscience Australia (http://www.ga.gov.au/interactive-maps/#/theme/minerals/map/geophysics). Grid coordinates in GDA 94)**

The geology of the east Lachlan (Figure 2) is characterised by the faulted contact between the Early Ordovician and the Mid-Late Silurian rocks (Lewis et. al., 1994). The overall geological framework strikes north-south, except for a rather dramatic east-west flexure in the major geological boundary between the Silurian and Ordovician formations. Tertiary basalt forms a thin veneer over a characterised by numerous open folded anticlinorial and synclinorial zones, which are bounded by both east and west dipping reverse faults (Foster and Gray, 2000). substantial portion of the region. This basaltic coverage makes traditional regional-scale mineral exploration approaches less effective thus impeding the systematic exploration of resources in the area (Glen and Lewis, 1994).

The east Lachlan province has been intermittently intruded by numerous granites and granodiorites during the Silurian and Early Devonian. The target deposit areas are situated close to the western extremity of the Bega Batholith, which is the largest batholith mapped in the Lachlan Fold Belt. The batholith is composed of more than 130 intrusive units, such as Silurian and Devonian I-type granites (Glen and Lewis, 1994).

The Cooma region, host sequence

Major stratigraphic sequences in the Cooma region range from Early Ordovician to Late Devonian age (Figure 2). The geology is dominated by an Early Ordovician – Late Silurian contact sequence, which is composed of groups such as the Bendoc, Yalmy and Bredbo Group. As described by Lewis and Glen (1994), these Groups encompass mainly shallow water sedimentary rocks and I-type volcanic fill of the Ngunawal Basin.
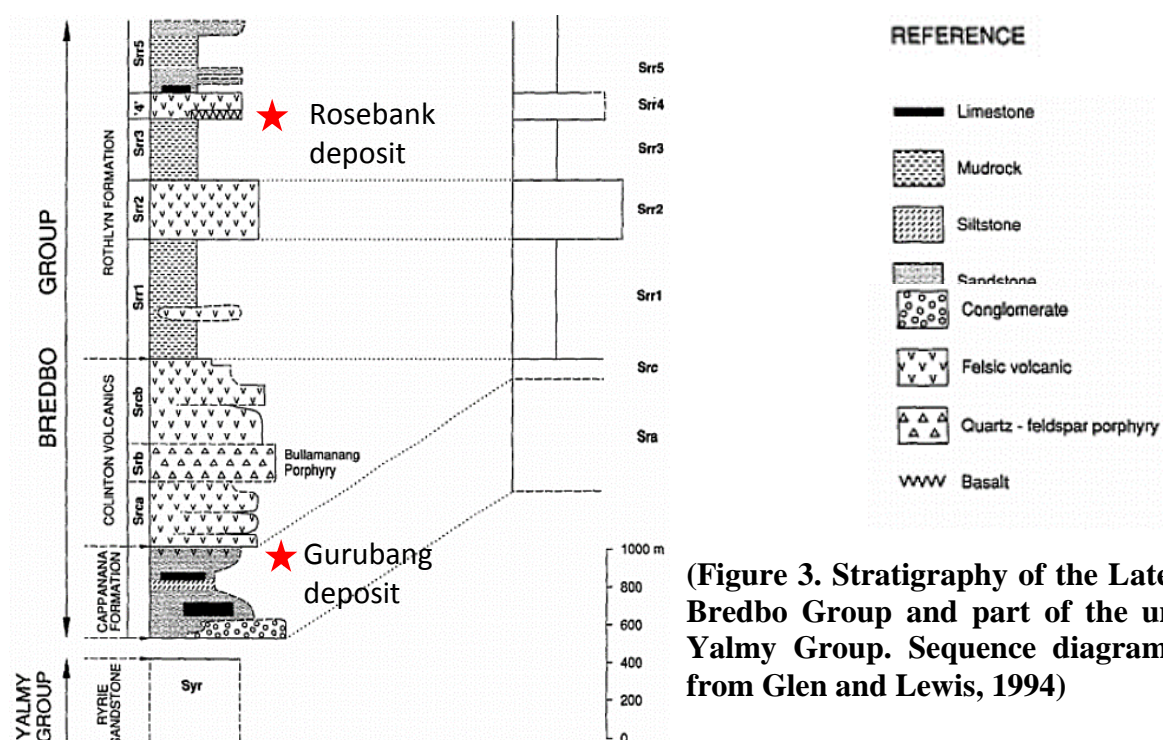
(**Figure 3. Stratigraphy of the Late-Silurian Bredbo Group and part of the underlying Yalmy Group. Sequence diagram sourced from Glen and Lewis, 1994**)

Base metal occurrences in the Cooma region and surrounding districts

Since the initial discovery of placer gold along the Numeralla River in 1858, the Cooma region and surrounding districts have undergone extensive exploration in the hopes of locating profitable mineral occurrences. A recent geological report by Smith Engineering (2015), suggests that the mineralisation in the district is minor but still significant enough to warrant further exploration. There are numerous small-scale base metal deposits (Figure 4), that are located within the Cooma region. Such deposits include, the Glenfergus Prospect, Woodend Prospect, Skidmore (North and East) Prospect, and the Square Range Prospect. These deposits vary in scale and contain base metal commodities such as copper, zinc and lead.
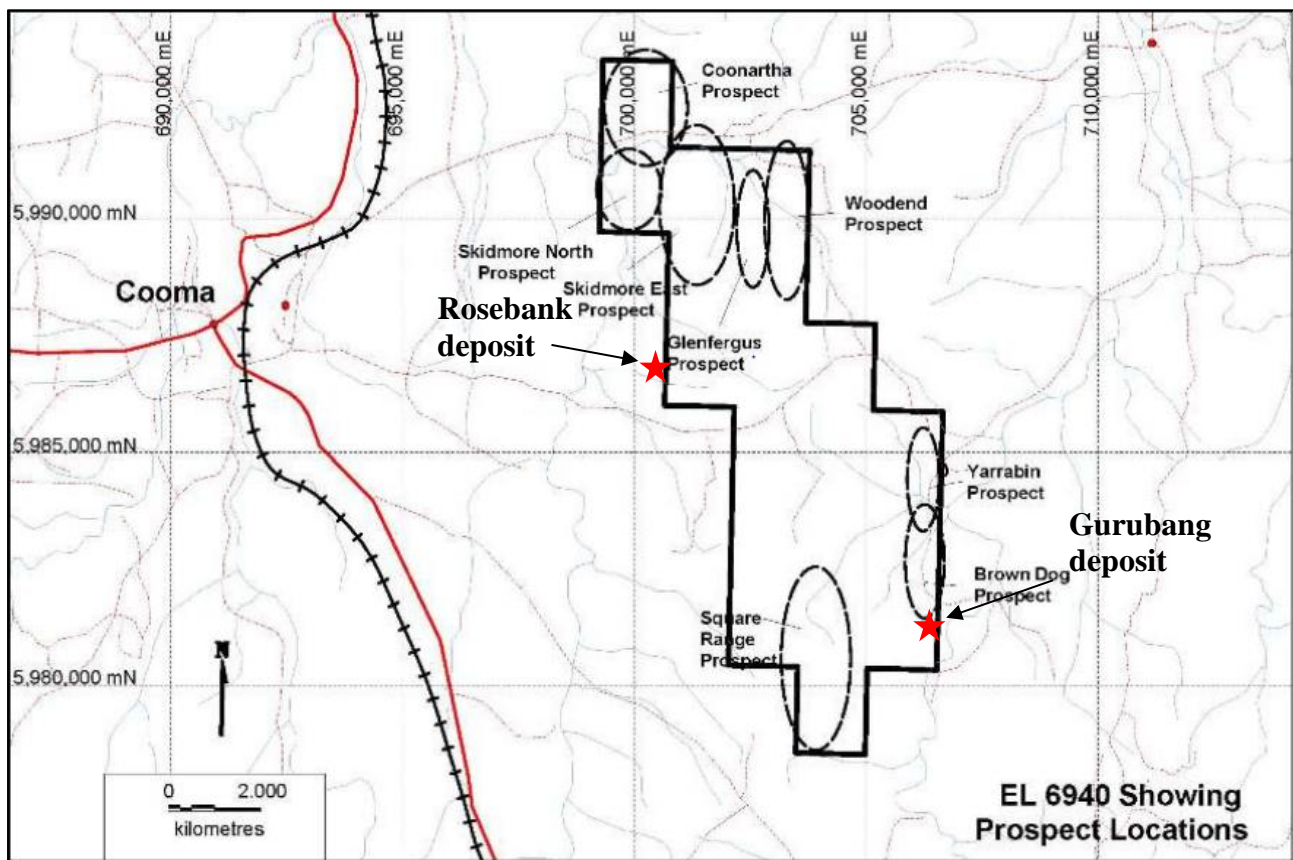
(Figure 4. Exploration license 6940 showing prospects located close to the study sites. Image sourced from Smith Engineering Systems (2015))

Common features of VHMS deposits

VHMS deposits are known to occur in the east province of the Lachlan Fold Belt. They are primarily hosted in mid-late Silurian felsic volcanic, volcaniclastic and sedimentary rocks (Ashley, Lawie, & Scott, 2001). VHMS mineralisation (Figure 5), is generally zoned, with massive to disseminated pyrite (+/- chalcopyrite) in the surrounding footwall, which grades into massive or banded $Zn - Pb - Cu$ ($\pm$ $Ag - Au$) sulphide-hosted metals. These deposits typically form in marine tectonic settings where a strong temporal and spatial relationship exists between magmatism and

hydrothermal venting (Galley, Hannington, & Jonasson, 2007; Slack et. al., 2003). Such settings are found in extensional oceanic seafloor spreading ridges, volcanic arcs (along oceanic and continental margins), and related back-arc basins (Morgan and Schulz, 2012).

Typical VHMS dimensions range from 100 to 500 m. Morgan and Shulz (2012) suggests that these large dimensional variations reflect diverse parameters, such as the duration and nature of sub-seafloor hydrothermal

(Figure 5. Primary mineral zonation around a typical mound VHMS deposit with a stock-work stringer zone. Diagram sourced from McQueen, 2005).

activity, structural and/or volcanic controls on mineralisation, extent of post-ore deformation and/or erosional preservation, and ore mineral grade. The vertical extent of a VHMS mineral horizon is controlled by post-depositional deformation. For relatively undeformed deposits, typical vertical extents are in the order of tens of metres. The greatest extents occur in deformed tabular and sheet-like deposits that dip steeply to almost vertical. Feeder zones also vary in vertical extent and range from tens to hundreds of metres long, depending on exhalative processes (Morgan and Schulz, 2012).

VHMS deposits have a wide variety of morphologies that typically reflect the original hydrothermal shapes, or alternatively, preserve varying degrees of post-deposition deformation such as folding or faulting. In regions of minimal deformation, deposits can be found as lenses, sheets, mounds, stock-work and disseminated (Morgan and Schulz, 2012). Mound deposits are the more commonly found deposit, in that the main mineral accumulate occurs directly over the central stock-work feeder zone. Sheet-like or lens deposits are characterized by horizon lengths exceeding the overall thicknesses of the body and that each layer shows broadly similar geometries. Stock-work or disseminated deposits occur in the footwall of sulphide-rich deposits and represent the hydrothermal feeder zone through which fluids migrated towards the paleo-seafloor (Morgan and Shulz, 2012).

Geophysical characteristics of VHMS deposits

VHMS deposits typically have a strong geophysical contrast with the surrounding host rock, due to the substantial difference in chemical and physical properties. Such properties include density, magnetic susceptibility or remanence, gravity, electrical conductivity or resistance, and acoustic
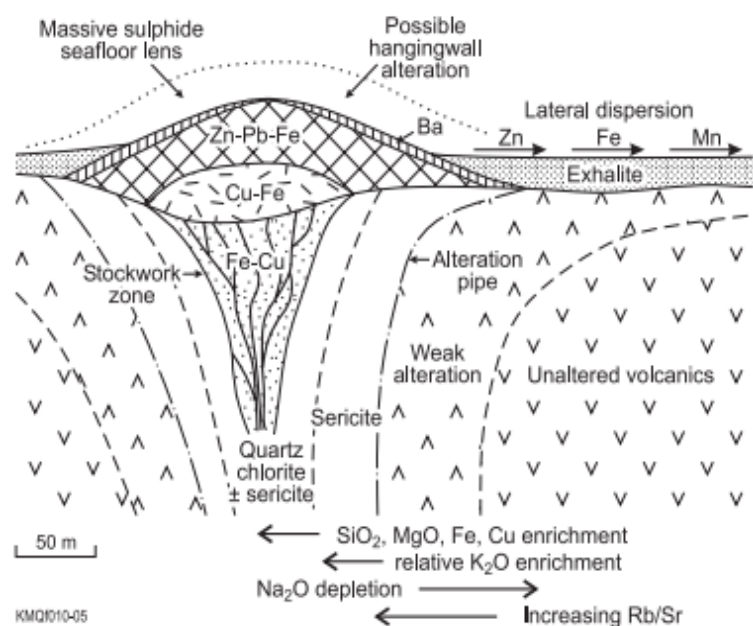
velocity. In terms of exploration, contrasting properties become direct detection vectors (Ford et. al., 2007).

According to Ford et. al. (2007), the most common sulphide mineral in VHMS deposits is pyrite, which is often associated with secondary sulphide minerals such as pyrrhotite, chalcopyrite, sphalerite and galena. Other non-sulphide minerals including magnetite, hematite and cassiterite can also be present. The noted minerals have relatively high magnetic and specific gravity values, relative to the typical host geology. VHMS deposits generally have high conductivities, exceeding 5×10^{-3} S/m (siemens per meter) compared to igneous, metasedimentary and sedimentary rocks, which have values ranging from <1 mS/m (millisiemens per meter) to 500 mS/m (Dentith and Mudge, 2014).

1.5 GEOPHYSICAL SIGNATURE OF THE COOMA REGION

The 1st vertical derivative (1VD) of the total magnetic intensity map (TMI, Figure 6), reveals the magnetic response of the geology of the Cooma region. It indicates that the Gurubang deposit is associated with a significant magnetic anomaly and is situated along the western margin of a large-scale magnetic feature. In contrast, the map shows that the Rosebank deposit is not associated with any magnetic signatures.

To the east of the deposit sites are two broad magnetic anomalies. These anomalies are characterized by their high magnetic signatures and elliptical shapes, which extends north-south. These types of anomalies are typically associated with intrusions, which according to Glen and Lewis (1994), the region did experience during the Devonian. The two intrusive bodies are most likely associated with the hidden plutonic intrusions of the Bega Batholith.

Towards the south-west of the deposit sites, are numerous irregular magnetic anomalies that appear to cluster in the south and become more parallel as they stretch towards the north. Geological interpretation (Figure 2), indicates that these features are related to the overprinting basaltic unit that erupted during the Cainozoic/Tertiary period. Along the western margin of the southern basaltic cluster, lies a circular anomaly with a similar magnetic signature to that of the basaltic unit. This anomaly may be indicative of the volcanic origin of the Tertiary basalt of the immediate region. A small section of the Rosebank deposit area is covered by this basaltic unit (Nagy, 1977).

The 1 VD total magnetic intensity map also indicates the presence of major and minor faults, such as the major Numeralla (F_1) and Murrumbidgee I-S fault (F_2). These structures influence the geological framework of the deposit localities (Glen and Lewis, 1994). The faults vary in size, in that some appear to extend for around $10 - 20$ km, while others only a few hundred meters. The majority of fault structures on the map trend north-south. However, crosscutting faults are present such as CF,

shown on the TMI map, which suggests that at some point during the formation of the present-day Lachlan, there was a change in the direction of regional compression, whereby faults of varying orientation were created (Foster and Gray, 2000).
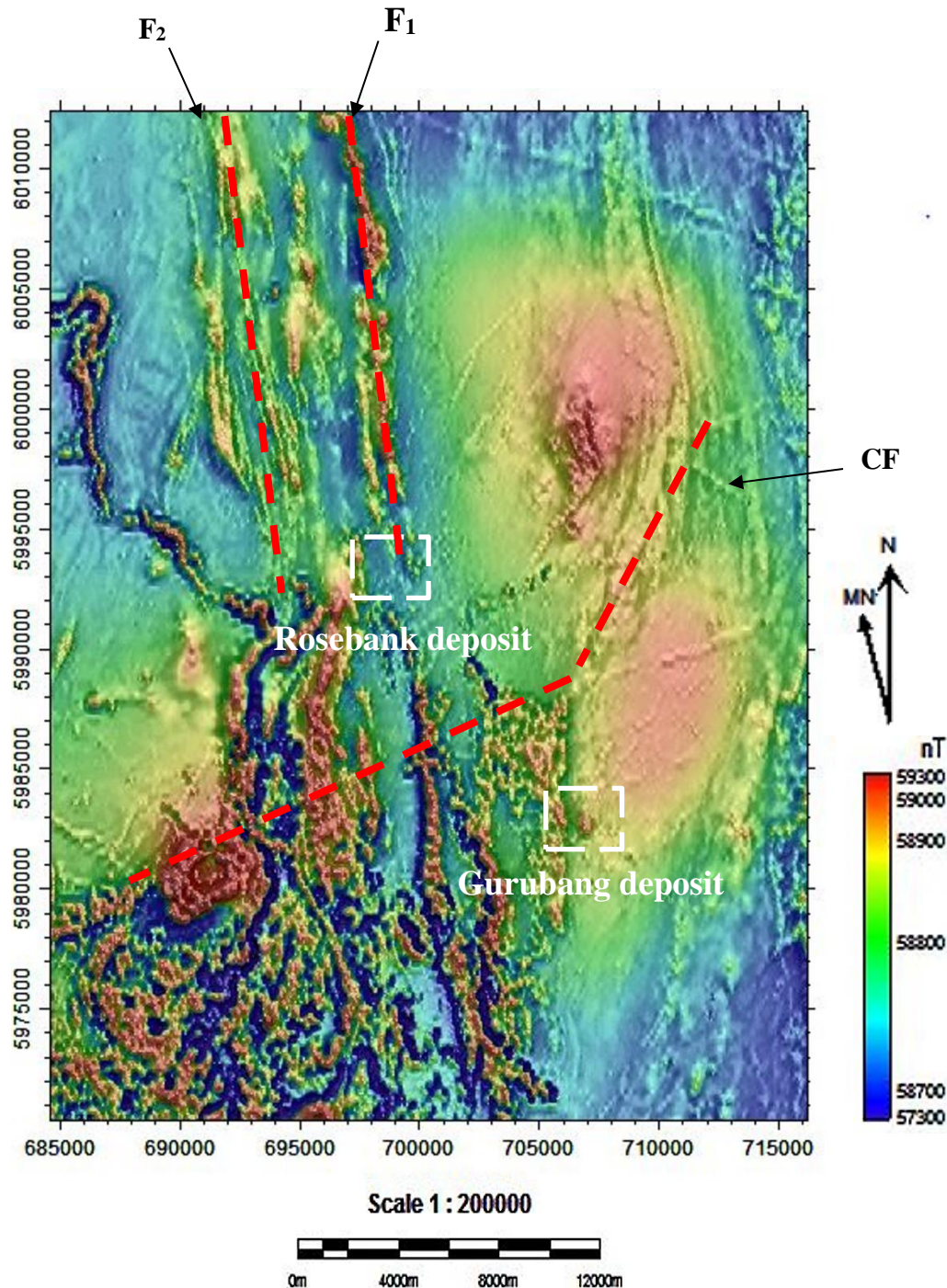
(Figure 6. First vertical derivative of the TMI map showing the geophysical response associated with the Cooma region and surrounding districts. F_1 and F_2 are major fault structures. CF represents a major cross-cutting fault. Data is based on the GDA94 regional airborne magnetics sourced from GADDS (www.geoscience.gov.au/geophysical-data-delivery).)

CHAPTER 2

STUDY LOCALITIES AND RESEARCH METHODS

2.1 INTRODUCTION

This chapter describes two well studied small-scale base metal occurrences, the Gurubang and Rosebank deposits, in the Cooma region of south eastern NSW. It summarises the field localities and past exploration work and describes the specific survey procedures and methods used to complete this study. The specific geophysical methods used include the time-domain electromagnetic, magnetic, and gravity methods. Magnetic susceptibility and density analyses were carried out on the collected rock samples from both deposit sites.

2.2 LOCALITIES AND AREA DESCRIPTIONS

Specified site selection (Figure 7 a and b on pg14) was based on mineral exploration work performed prior to the commencement of this thesis.

Gurubang deposit

The Gurubang (south) site, (Figure 7 a), is located 15 km east of Cooma, NSW, alongside the Numeralla River. The land is privately owned and utilised for agricultural purposes, primarily for sheep and cattle. The topography of the target area is relatively flat with a moderate coverage of native trees and small shrubbery. Non-geographic, cultural artefacts including boundary fencing and a single storage shed are located on site and have been accounted for during data acquisition and processing.

The deposit was first discovered by Aquitaine Australia Minerals during the mid-1970's. Numerous drillings were carried out across the prospect area, targeting two EM anomalies that were previously identified using a CRONE EM system. The diamond drilling (summarised in Table 1) intersected significant VHMS mineralisation hosted in an alternating sequence of limestone and shale. However, the base metal yield values were considered too low and no further investigation was undertaken (Wilson, 1994). Previous geological reports describe the mineralisation composition at Gurubang as disseminated and composed primarily of pyrite and pyrrhotite with minor sphalerite and other sulphides (Ellito, 1984; Horsburgh 1984). According to Gunn and Dentith (2014), Gurubang is a pyrrhotite-rich, sub-economic Cu – Zn deposit containing approximately 20 Mt of mineralisation. This mineralisation occurs in zones, in that massive sulphides are underlain by a layer of disseminated mineralisation and are overlain by a magnetic pyrrhotite-rich 'ore equivalent' horizon.

Rosebank deposit

The Rosebank site (Figure 7 b) is situated around 10 km northeast of Cooma, NSW. Much like the Gurubang site, the area is privately owned and primarily used for agricultural purposes. The topography is relatively flat and contains a shearing shed, electrified fencing, pockets of vegetation, waterways and waterholes, and the remains of a buried mineshaft. The Rosebank deposit is a follow-up investigation of an old prospectors' shaft, the Rosebank Mine, which was operational at the turn of the 20th century. Cominco Resources carried out drilling (Table 1) in the immediate Rosebank area, targeting an EM anomaly. The core identified a lens of black 'graphitic' shale, which contained high quantities of pyrite with minor pyrrhotite. Cominco also performed assays on outcropping rock samples, which indicated spotty concentrations of high level Pb, Zn and Cu. Due to the low concentrations of base metal material no further investigation was undertaken. Accoding to Herzberger and Barnes (1976), the mineralisation of the Rosebank deposit occurs as a VHMS-related vein or stringer, occupying a shear, within a slate unit. However the dimensions and ore mineralogy of the deposit are not documented.

2.3 FIELD PROCEDURES

In mineral exploration, ground-based geophysics is generally used as a follow-up method to airborne surveys. The aim of carrying out ground-based surveys is to obtain high-resolution data that is crucial in effectively evaluating ore deposits. This study involves the use of three ground-based methods: time-domain electromagnetic (TDEM); magnetic, and gravity.

The procedural approach for the range of geophysical methods followed the 'Basic Ground Field Procedures' outlined in Dentith and Mudge (2014). Such procedures include: (i) profiles running perpendicular to geological strike; (ii) tight recording and station spacing, and; (iii) tight line spacing. Therefore, various tightly spaced, high-resolution surveys (Figure 7 a and b) were carried out across both project areas. This involved: (i) profiles traversing east-west (perpendicular to north-south strike of underlying geology); (ii) 5 m station spacing, and (iii) 20 – 50 m line spacing.

2.4 GEOPHYSICAL METHODS

Ground-based time-domain electromagnetic (TDEM) method

The electromagnetic (EM) method directly detects variations in rock conductivity. The EM method is most sensitive to good conductors, such as sulphide mineralisation (Dentith and Mudge, 2014). There are two classes of EM systems: Time-domain (TDEM) and frequency-domain (FDEM).

(Table 1. Summarised drill hole information sourced from the available drill logs for the Gurubang and Rosebank deposits.)

Drill hole	Bearing (degrees from true north)	Inclination from horizontal (°)	Depth to mineralisation (m)	Mineralisation thickness (m)	Description of mineralised horizon	Average measured magnetic susceptibility (SI)	Average measured density (g/cm³)	Conductivity range (S/m)	Reference
Gurubang deposit									
BDG - 102	060	-61	55.6	1.02	Dark siltstone - chert with pyrrhotite: Pyrrhotite and pyrite beds within a sedimentary breccia.	0.04	3.24	150 - 300	(Castle, 1976; Argaud, 1976, and Cooke, 1977)
BDG - 103	059	-61	129.6	7.5	Massive sulphide section: Sulphide 80 - 85%, mostly pyrrhotite with chalcopyrite 2 - 3% and sphalerite 5 - 7%, minor pyrite.	0.02	3.74	150 - 230	(Castle, 1976; Argaud, 1976, and Cooke, 1977)
BDG - 104	245	-50	82.2	8.4	Massive sulphide section: Overall sulphide 80%, of which 60% is pyrrhotite, 30% is pyrite and 2 -3 % is chalcopyrite.	0.04	3.92	100 - 240	(Castle, 1976; Argaud, 1976, and Cooke, 1977)
BDG - 105	245	-70	(i) 95.7 (ii)159.4	(i) 10.2 (ii) 59.0	Massive sulphide section: Dominantly pyrrhotite, pyrite with minor chalcopyrite and sphalerite.	n.d.	n.d.	n.d.	(Castle, 1976; Cooke, 1977)
Rosebank deposit									
PH - 1	081	-61	28	15.5	Shale, black section: Pyrite ranges from 5 - 25% with spotty metal concentrations	n.d.	n.d.	n.d.	(Nagy, 1977; Rabone, 1978)

High-resolution, ground-based TDEM surveys were carried out across the deposit areas (Figure 7 a and b). The surveys involved using a terraTEM Transient EM System that was connected to a set of grounded wires. The terraTEM system was powered using a single 24 V battery and allows for simultaneous sampling at 500 kHz of three component transient data. Basic TDEM field configurations are summarised by Nabighian and Macnae (1991).

The TDEM survey, across the Rosebank area, was carried out using a coincident loop configuration, whereby the transmitter (Tx) and receiver (Rx) coils are in the same position. Geometrically, the survey setup involved a 100 m x 100 m Tx-Rx loop size. Unfortunately, due to time constraints, only two 900 m east-west profiles were obtained in the area (250N and 350N). EM measurements were collected using a single 2048 stack approach, in that the transient system attained 2048 readings per station. It was noted during data collection that the field data was likely contaminated by noise, possibly due to the presence of electric fences, sferic interference or coupling induced by superparamagnetic material.

An in-loop TDEM survey, where by the Rx coil is placed in the centre of the Tx loop, was initially proposed for the Gurubang deposit. This setup was aimed at limiting the amount of noise contamination, as was evident in the Rosebank dataset. However, it was found that the in-loop Rx equipment was damaged beyond instant repair, prior to the commencement of the survey. Therefore, the coincident loop was used to collect the TDEM data. The process of acquiring measurements in this survey involved using a 4 x 512 stack approach. Having the 4 sample bins of 512 stacks instead of 1 bin of 2048 stacks, dramatically reduced the amount of noise in the dataset. A total of 4 x 600 m east-west profiles were obtained over the Gurubang area.

Ground-based magnetic survey

Magnetic surveys measure spatial variations in the Earth's magnetic field, which are generally induced by buried magnetic material. The method is fundamental in determining the strength and shape of crustal magnetic bodies (Dentith and Mudge, 2014). Prior to commencing the ground-based magnetic survey, relative magnetic susceptibilities were acquired from in-situ lithologies across the deposit areas. The purpose of this preliminary study was to assess for any baseline variation in magnetic susceptibility across the deposit areas. A magROCK 750 Hz handheld magnetic susceptibility meter was used to collect the in-situ measurements. The sensitivity of the instrument is 1×10^{-5} SI and was operated in static mode.

On completion of the preliminary magnetic study, a ground-based magnetic survey was carried out across the two deposit localities (Figure 7 a and b). Diurnally corrected magnetic readings
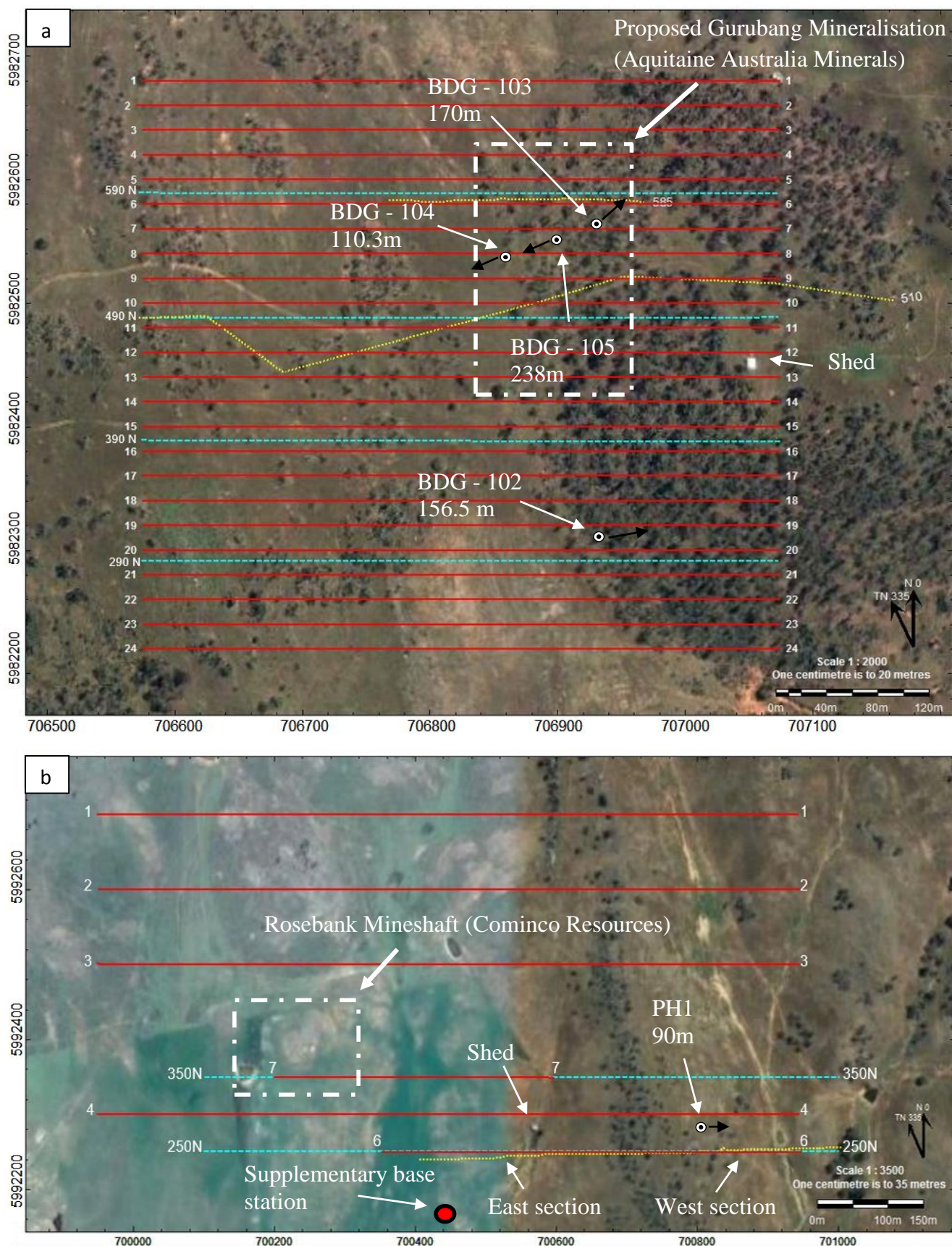
(Figure 7. a & b are satellite photographs of the two deposit localities (https://www.google.com/earth/).
a. Gurubang deposit site.
b. Rosebank deposit site.
East-west trending survey lines include: (RED) magnetic; (BLUE) TDEM, and; (YELLOW) gravity.
Drill holes are marked with approximate bearing and total depth. Grid coordinates in MGA94.)

were acquired using two G 856 Memory-MAGTM Proton Precession Magnetometers (accuracy of ~1 nT) and a single G 858 MagMapper Caesium Vapour Magnetometer (accuracy of ~0.01 nT). During each survey period, a G 856 magnetometer was used as the base station. The two remaining magnetometers were then used to obtain field measurements.

A total of 6 profiles, trending east-west perpendicular to geological strike, were acquired across the Rosebank deposit locality (Figure 7 b). The survey initially involved 4 x 1000 m profiles at 5 m station spacing and 50 m line spacing. The addition of the shortened profiles (1 x 300 m, and 1 x 200 m lines at 5 m station spacing and 20 m line spacing) was due to a follow-up investigation of a detected TDEM anomaly.

Twenty-two profiles were completed over two different acquisition periods for the Gurubang deposit site (Figure 7 a). The profiles extend east-west, perpendicular to geological strike, for approximately 600 m at 5 m station spacing and 20 m line spacing.

Ground-based gravity survey

The gravity method is typically used in follow-up investigations of magnetic and electromagnetic surveys. The purpose of carrying out a gravity survey is to measure for spatial variations in the Earth's gravitational field caused by differences in rock densities (Dentith and Mudge, 2014).

Ground-based gravity surveys were carried out over the two deposit areas (Figure 7 a and b). The instruments used to collect the gravity measurements were a Scintrex CG-3 and Scintrex CG-5 gravimeter. Due to the university acquiring the CG-5 gravimeter after surveying over the Rosebank deposit, the equipment was only used in the Gurubang deposit survey. Positioning and elevation of gravity stations were measured using an Ashtec Real Time Kinematic (RTK) satellite navigation, which has an accuracy of ~ 1cm. A base station, Ashtech Z – Xtreme duel frequency receiver, and a mobile unit, Ashtech Geodetic IV antenna receiver, were used in this survey. The relative positions and elevations were later corrected using the positioning from Geoscience Australia's AUSPOS – Online GPS processing service (http://www.ga.gov.au/scientific-topics/positioning-navigation/geodesy/auspos) to accurately locate the GPS base station.

A single east-west profile was carried out over the Rosebank deposit area. Line selection was based on a follow up investigation of the TDEM results. Of note, is that there was an uneven distribution in station spacing, greater than 5 – 10 m, due to a small stretch of dense bush area inhibiting a continuous collection of measurements.

The profile was then divided into two sections; east and west of the bush area (Figure 7 b). The eastern stations extend for approximately 300 m, while the western stations extended for approximately 200 m. A supplementary base station (Figure 7 b) was established to tie both east and west stations.

Two east-west profiles were carried out across the Gurubang project area. A 200 m profile was obtained using the CG-5 system, while a 600 m profile was measured using the CG-3 system. The station distribution was about even, between 5 m – 10 m apart. Line selections were based on TDEM results and EM results from the previous mineral exploration work.

2.5 LABORATORY PROCEDURE

Sample preparation

Twenty-five rock samples, fourteen (Rb01 – 14) from the Rosebank site and eleven (Gb01 - 11) from the Gurubang site, were collected for the purpose of a physical property analysis (density and magnetic susceptibility). Each sample is representative of the contrasting lithologies that comprise the deposit areas. Eleven of the twenty-five (Rb01 – 9, Gb09 and 11) rock samples were prepared using the rock cutting saw at Macquarie University, North Ryde, while the remaining fourteen samples (Rb10 – 14, Gb01 – 08 and 10) were prepared using the diamond drill at the CSIRO Rock Magnetism Laboratory.

Magnetic susceptibility

Magnetic susceptibility is largely dependent on the type and concentration of magnetic minerals within a rock. Volume corrected apparent magnetic susceptibility readings were measured for the twenty-five samples obtained from the deposit areas (Table 2). Susceptibilities were measured using a Sapphire Instrument SI2 susceptibility meter located at Macquarie University. The meter has an accuracy of 1×10^{-5} SI units. Each magnetic susceptibility value is an average of multiple (generally three specimens from the same lithology) readings.

Density analysis

Density measurements were obtained for the twenty-five rock samples (Table 2). Measurements were achieved using a Precision Mettler Electronic Balance at Macquarie University. The balance is accurate to 1×10^{-4} g. In preparation for the density measurements, the density of the liquid (ionized distilled water) was calculated (D_l). Samples were then weighed three times: weight in air (W_A); weight saturated (W_S), and weight in liquid (W_L). The obtained values were then processed to calculate the bulk density of each sample. Saturated measurements had been obtained

after the samples had been submerged in water for twenty-four hours. Each density measurement is an average of multiple (generally three specimens from the same lithology) readings.

2.6 VISUALISATION AND MODELLING OF FIELD DATA

The graphic visualisation and geological modelling of the attained geophysical field data was achieved using a combination of computational software packages, including: ModelVision; Discover PA; MapInfo Discover; ER Mapper; Maxwell, and TEMDISP.exe. Coordinates are in the Geocentric Datum of Australia (GDA94), grid coordinates are in Map Grid of Australia (MGA 55).

1. ModelVision (http://www.tensorresearch.com.au)
2. Discover PA, MapInfo Discover (http://www.pitneybowes.com)
3. ER Mapper (http://www.hexagongeospatial.com)
4. Maxwell (http://www.electromag.com.au)
5. TEMDISP.exe (pers. comm. Steve Collins)

(Table 2. Petrophysical values measured in rock samples collected across the Gurubang and Rosebank deposit localities.)

Lithology	Magnetic Susceptibility (x 10^{-5} SI)	Density (g/cm^3)
Gurubang deposit area		
Fossiliferous/Massive limestone	45	2.69
Coarse sandy-siltstone	101	2.63
Red - pink, highly weathered, ferruginous gossan	160	2.63
Dark red - black, highly ferruginous gossan	213	2.70
Moderate to fine grained basalt	213	2.86
Lighter colour, ferruginous tuff	88	2.66
Tuffaceous, sulphide-rich ferruginous quartzite-siltstone	480	2.96
Ferruginous, darker - red bands present (ironstone) gossan	365	2.83
Limestone breccia	207	2.76
Dark gossanous material, possible manganese inclusion	236	2.83
Ferruginous ironstone with pyrrhotite-rich dyke intrusion	720	3.69
Rosebank deposit area		
Highly ferruginous shale	249	2.61
Ironstone	24	2.63
Fine grained siltstone	257	2.65
Felsic coarse-grained tuff	-3	2.60
Red – pink ferruginous siltstone	158	2.27
Vein-rich quartzite	55	2.62
Very fine-grained shale	261	2.69
Fragments of graphitic shale from percussion drill (PH-1)	963	2.50
Fine grained quartz-rich sandstone	202	2.63
Coarse grained shale	103	2.66
Tuffaceous siltstone	36	2.34
Cherty sandstone	291	2.81
Coarse-grained sandstone	10	2.58
Fine grained shale	87	2.63

CHAPTER 3

GEOPHYSICAL SIGNATURES OF BASE METAL DEPOSITS

3.1 INTRODUCTION

This chapter outlines the geophysical observations made across the Gurubang and Rosebank deposit localities. This study has greatly increased the amount of high-resolution data available for the two study sites. The new data is used to evaluate the ore bodies and better understand the geological framework at a local and prospecting scale. The Gurubang deposit is first examined due to the abundant information regarding the location of the mineralised horizon, provided by the drill logs obtained during previous drilling (Castle, 1976 and Cooke, 1977). This will allow us to observe first-hand the geophysical response produced by these small-scale base metal deposits. Results from the high-resolution, ground-based magnetic, time-domain electromagnetic (TDEM) and gravity surveys, are outlined in the following section.

3.2 GURUBANG DEPOSIT

Ground-based magnetic survey

The high-resolution, ground-based magnetic survey from the Gurubang study area, was conducted at different times using two different magnetometer systems. This lead to some minor discrepancies in the magnetic intensity on common sections, which was later rectified by implementing an offset (based on the total variation between the two common sections) to some of the acquired data. The magnetic anomaly map (Figure 8 a) was compiled using the Discover PA software. It was necessary to apply an upwards continuation (10 m) grid filter to remove the superficial magnetic noise produced by near surface features. Magnetic artefacts, such as those induced by fencing, were identified via cross referencing position and manually filtered from the observed dataset.

In total, the magnetic response ranges from -323 – 2276 nT. Anomaly A (Figure 8 a), is a broad, weakly-elongate feature, showing a high magnetic response ranging from 158 - 511 nT. The anomaly extends north for approximately 200 m and has a width of about 100 – 150 m. Smaller magnetic anomalies are located just east of the larger anomaly A. Anomaly B is a relatively thin, 10 – 20 m response, that has a magnetic signature ranging from 210 - 616 nT. Its irregular elongate, flexing shape appears to trend north-south and differs from the more elliptical shapes of the surrounding responses. Anomaly C has a broad magnetic response, ranging from 109 - 341 nT, and an elliptical shape extending north-south.

In contrast to the strongly magnetic north, the data presents areas to the south with significantly low magnetic intensities. Anomaly D is located at the base of anomaly A and has a magnetic signature ranging from -179 - 323 nT and has a slightly rounded, irregular shape.
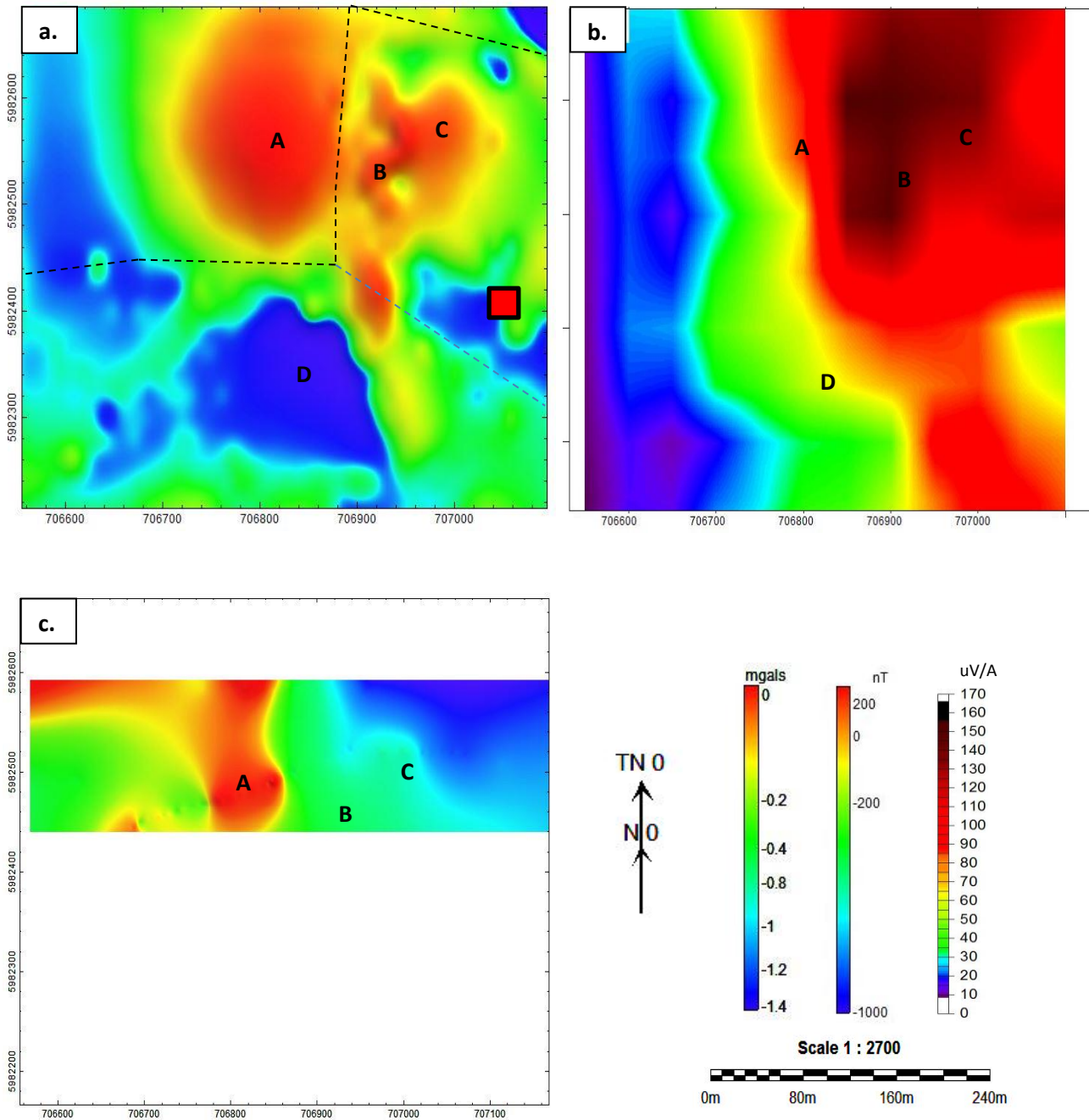
(Figure 8. a, b and c are visualised maps based on the geophysical datasets collected across the Gurubang area.
a. Upwards continued 10 m magnetic anomaly map.
b. Conductivity response amplitude map for channel 95.
c. Corrected bouguer anomaly map.
Boundary fence outlined with black dotted line, red box outlines storage shed. Grid coordinates are in GDA94.)

Ground-based TDEM survey

The conductivity response amplitude map (Figure 8 b), was visualised using the Maxwell software. Conductivity values appear to be higher (ranging from 90 -160 uV/A) in the east and lower (ranging from 10 – 60 uV/A) towards the west. The highest conductive response is shown in the northeast, which exceeds 160 uV/A.

The TDEM response profiles (Figure 9 a, b, c and d), were generated using the TEMDISP.exe program. Three discrete conductive responses, two mid-late (CC1 and CC2) and one early-mid channel time (CC3), were identified within the Gurubang deposit locality. Two of the three conductive responses (CC1 and CC2) are identified along profile 590N and 490N (Figure 9 a and b), while a single conductive response (CC3) is shown in the eastern section of profile 290 N (Figure 9 d). An early-channel time response is present in the eastern section of profile 390 N (Figure 9 c). This response is along strike of conductor CC3, but the signal was contaminated by noise and is difficult to identify.
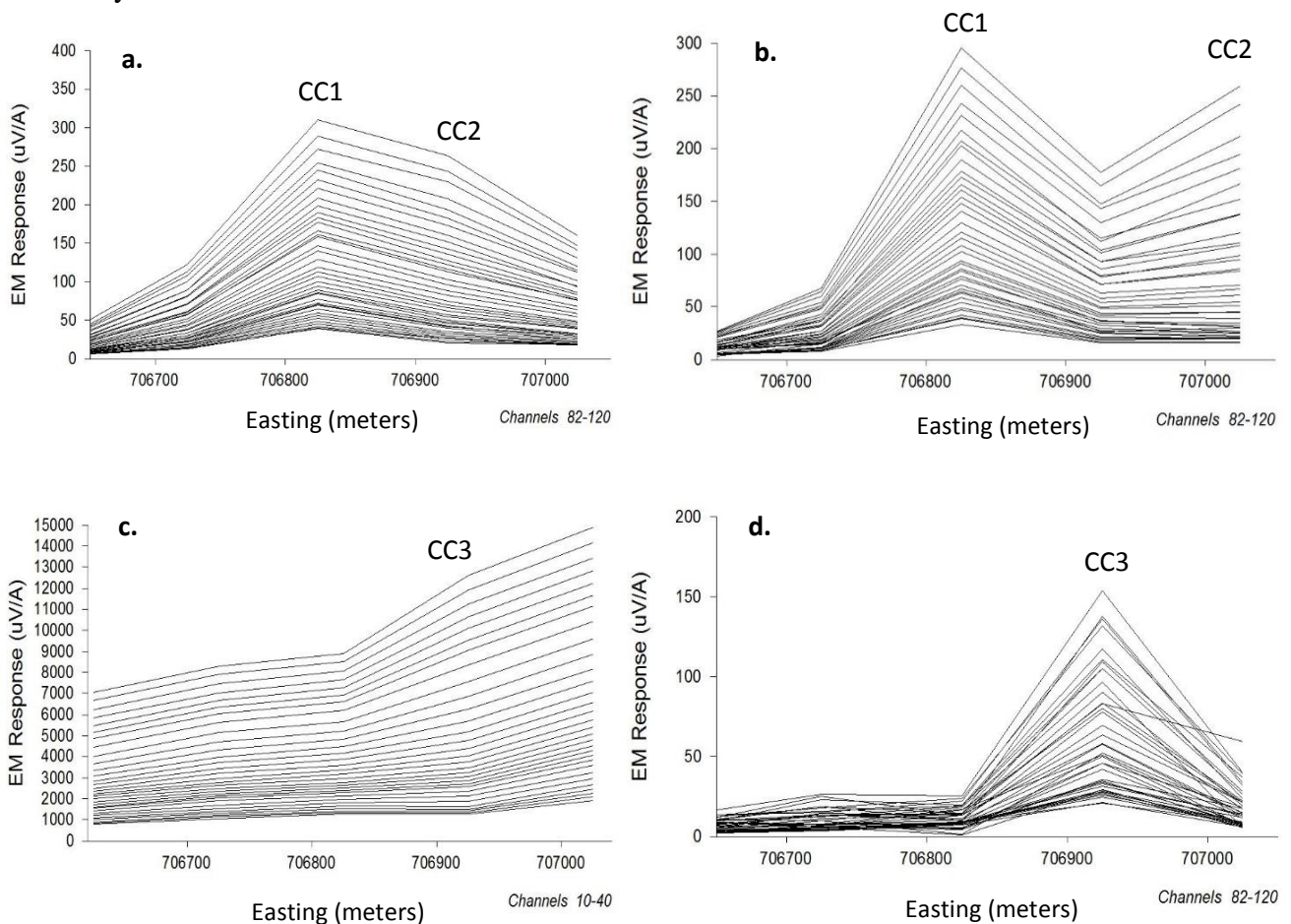

(Figure 9. TDEM profiles from the Gurubang project area.
a. 590N
b. 490N
c. 390N
d. 290N)

Ground-based gravity survey

Two high-resolution gravity profiles were conducted across the Gurubang deposit area using the two different gravimeters. Fortunately, there were no discrepancy between the two obtained datasets. The gravity map (Figure 8 c), was based on the gravity corrected Bouguer anomaly values obtained across the Gurubang deposit area. The total gravity response for the area ranges from -1.29 – 0.14 mgal (milligal). The map indicates a high gravity anomaly associated with anomaly A.

Bouguer anomaly profiles (Figure 10 a and b) were created using the ModelVision software. The profiles indicate an overall east-trending negative gradient, with the greatest response located between 706750E – 706850E (grid coordinates MGA 55), which is indicated as A on the gravity map.
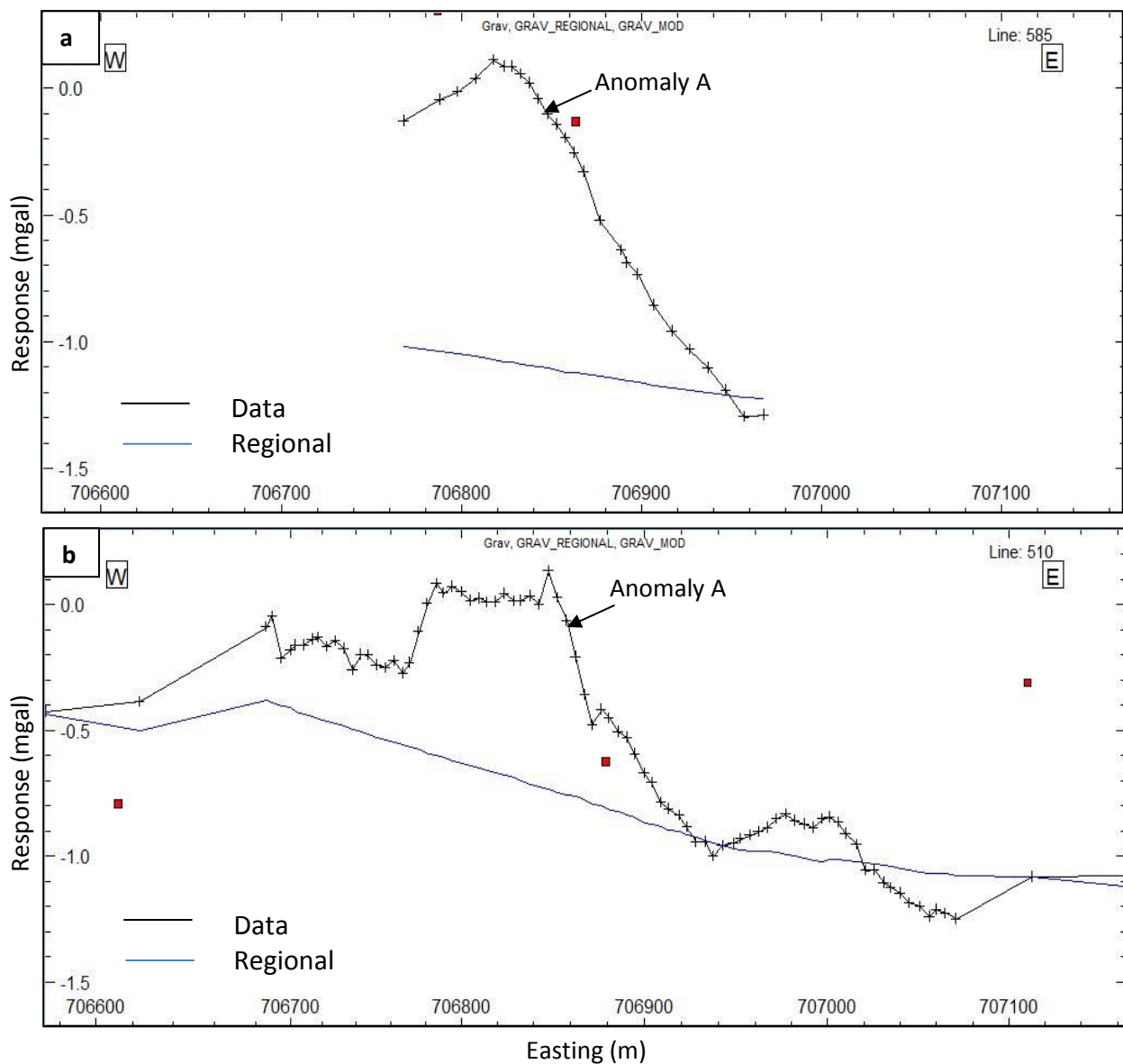

(Figure 10. a and b are two bouguer anomaly profiles obtained across the Gurubang area.
a. Line 585: Scintrex CG - 5 at 10 – 20 m station spacing.
b. Line 510: Scintrex CG – 3 at 5 m station spacing.
Regional gravity calculated using the acquired data indicated by the blue line.)

3.3 ROSEBANK DEPOSIT

Ground-based magnetic survey

The high-resolution, ground-based magnetic anomaly map (Figure 11), was based on the diurnally corrected magnetic dataset obtained across the Rosebank deposit locality. To remove the high-frequency near-surface noise, an upward continued 10 m grid filter was applied to the data. The magnetic data has a total magnetic response ranging from -158 – 136 nT.

Anomaly A, shown in the northwest corner of the anomaly map, has a magnetic response ranging from -22 – 136 nT. Anomaly A_1 (magnetic signature of -158 nT), has a slightly elliptical shape trending NNE – SSW for approximately 100 m. Two prominent responses, anomalies B and C, are situated in the eastern section of the surveyed area. Anomaly B has a magnetic response ranging from -13.8 – 31 nT and has an irregular elongate shape extending north-south. It has a broader shape to the north and appears to taper off as it moves further south. To the west of anomaly B is anomaly C, which has a relatively moderate magnetic response ranging from -44 – -22 nT. Anomaly C is a smaller anomaly and has an elliptical shape extending north-south. Located in the southwest section of the anomaly map is a horizontal magnetic response, anomaly D. This feature has a magnetic signature ranging from -28 – -5 nT and extends east-west, though it is truncated by the survey boundaries.
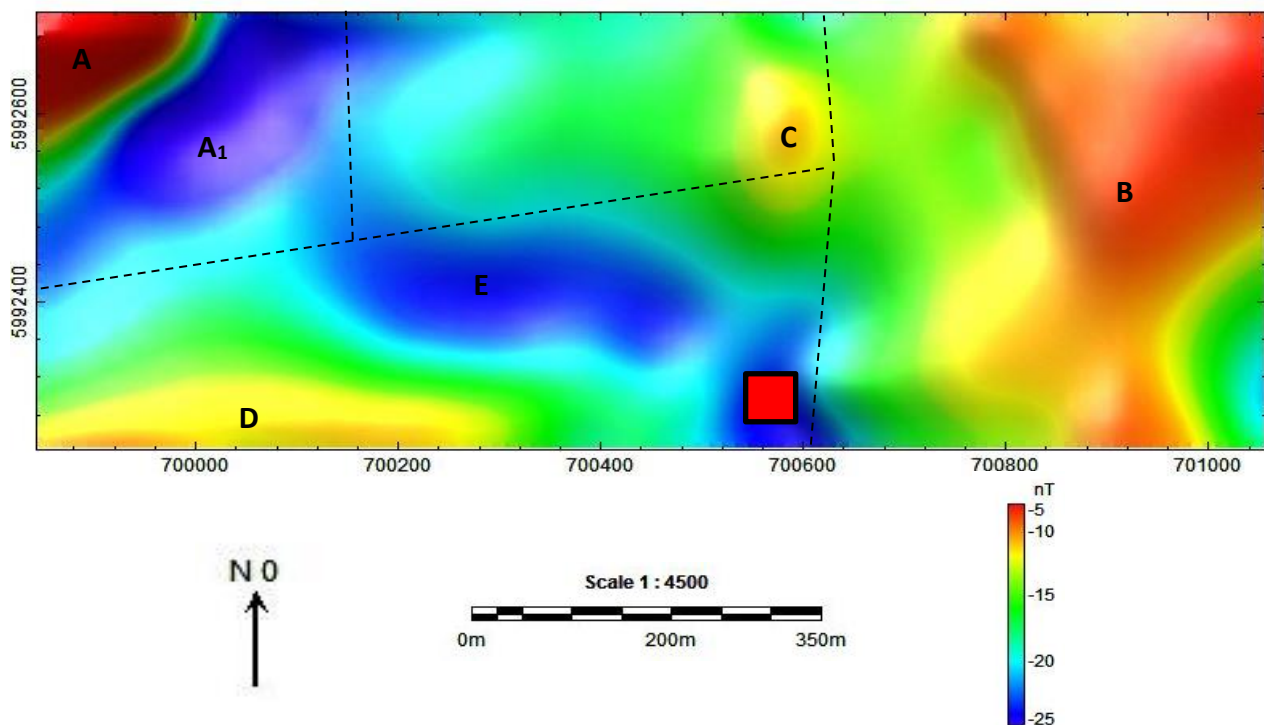

(Figure 11. Magnetic anomaly map of the Rosebank deposit locality. Primary anomaly features are marked using letters. Red square is the location of the shearing shed, black dotted lines is boundary fencing. Grid coordinates are in GDA94.)

The magnetic anomaly map presents areas of low magnetic signatures. Directly north of anomaly D is anomaly E. This response is a gridding artefact created by the software package due to the absence of data, which was caused by time constraints.

Ground-based TDEM survey

The TDEM profiles (Figure 12 a, b and c) were generated using the TEMDISP.exe and Maxwell software. The profiles are based on the TDEM dataset obtained across the Rosebank deposit locality. Unfortunately, due to time constraints only two east-west profiles were measured. The data was manually filtered to remove most of the noisy signal. The data presents two conductive anomalies; an early to mid-channel time (CC4) and a late-channel time (CC5). Profile 250N and 350N (Figure 12 a and b), indicate the presence of the early to mid-channel time conductive signature at around 700550 E (CC4). The late-channel time conductor (CC5) is situated in the eastern section (around 700900 E) of profile 250 N (Figure 12 c).
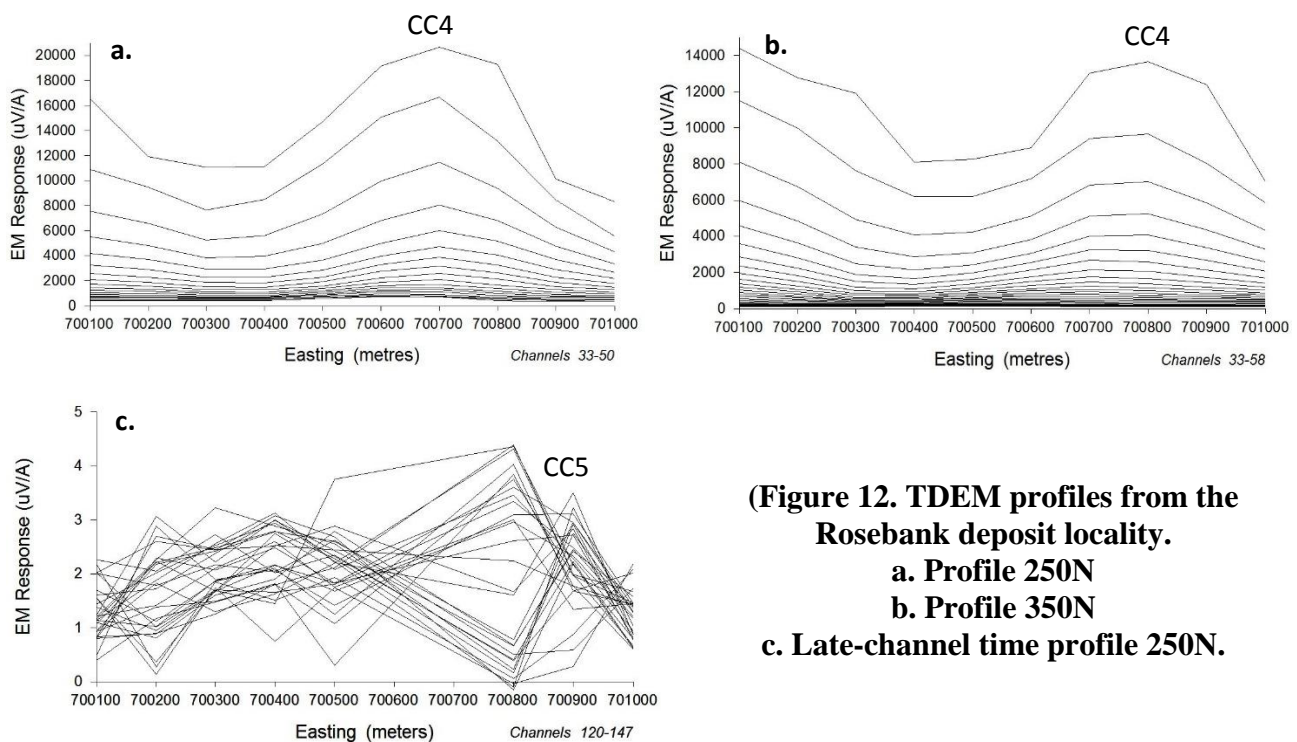
(Figure 12. TDEM profiles from the Rosebank deposit locality.
a. Profile 250N
b. Profile 350N
c. Late-channel time profile 250N.

Ground-based gravity survey

The gravity profile (Figure 13 a) was generated using the ModelVision software. It is based on the gravity corrected Bouguer anomaly dataset obtained over the Rosebank deposit locality. The profile appears to be dominated by an east trending negative gradient, ranging from $-0.20 - 0.25$ mgal, culminating in a prominent gravity low towards the central (i) and eastern zone (ii). Figure 13 b, was generated to compare the Bouguer anomaly profile to the magnetics anomaly dataset. Each dataset

runs across the same line, 250 N. Visual comparison of both datasets reveals a correlation between a magnetic high and gravity low in the eastern section (ii). The TDEM data does not contribute to the analysis of this profile data.
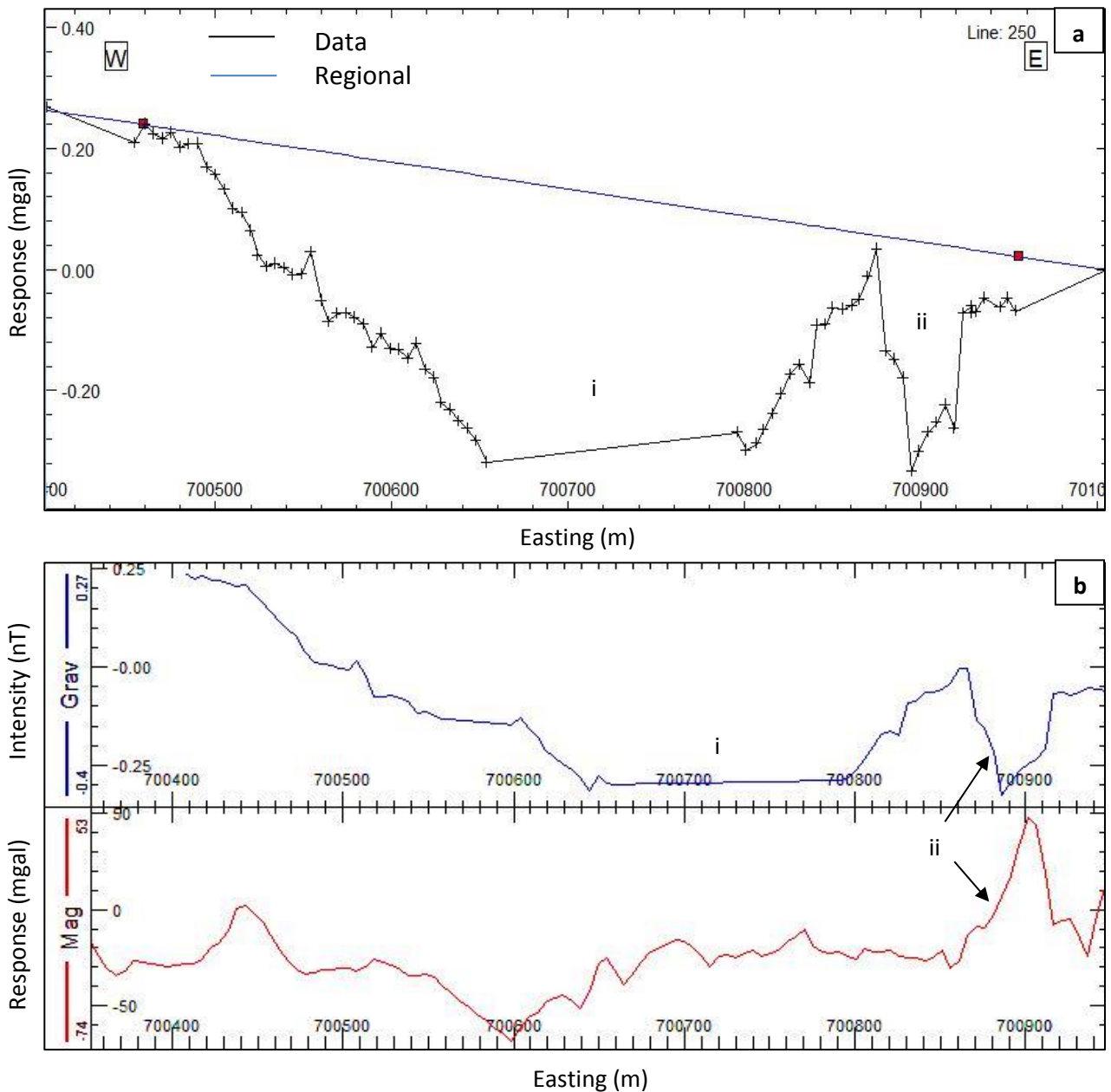
(Figure 13. a. Gravity corrected Bouguer anomaly profile for line 250N obtained across the Rosebank area. Black crossed line is the data, blue line is the regional gravity calculated via the acquired data.
b. Multitrack display showing the Bouguer anomaly gravity in blue and magnetics in red for line 250N)

CHAPTER 4

ADVANCED GEOPHYSICAL DATA MODELLING

4.1 INTRODUCTION

This chapter outlines the geophysical models generated to explain and evaluate the small-scale base metal deposits based on the obtained high-resolution geophysical data. In this respect, effective forward modelling of the results is carried out based on regularly shaped geometries and yield approximations to the known properties of the measured sources. Geological interpretations, petrophysical studies and drill core logs, performed during and prior to this study, were then used in interpreting and adapting the model parameters to determine outcomes.
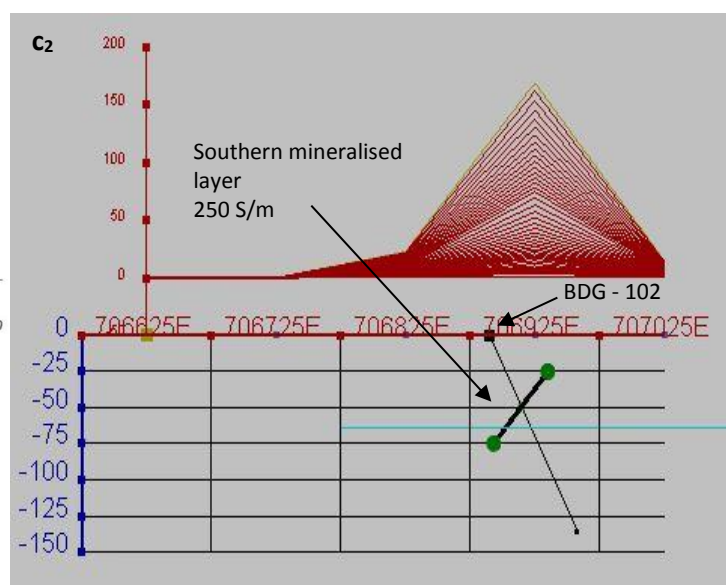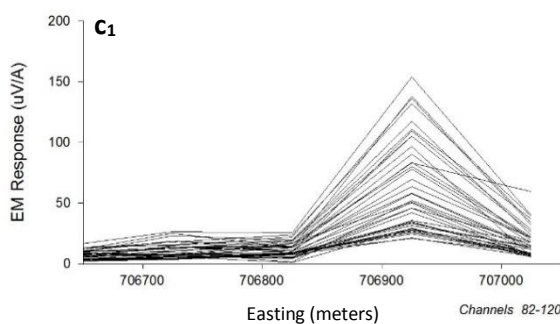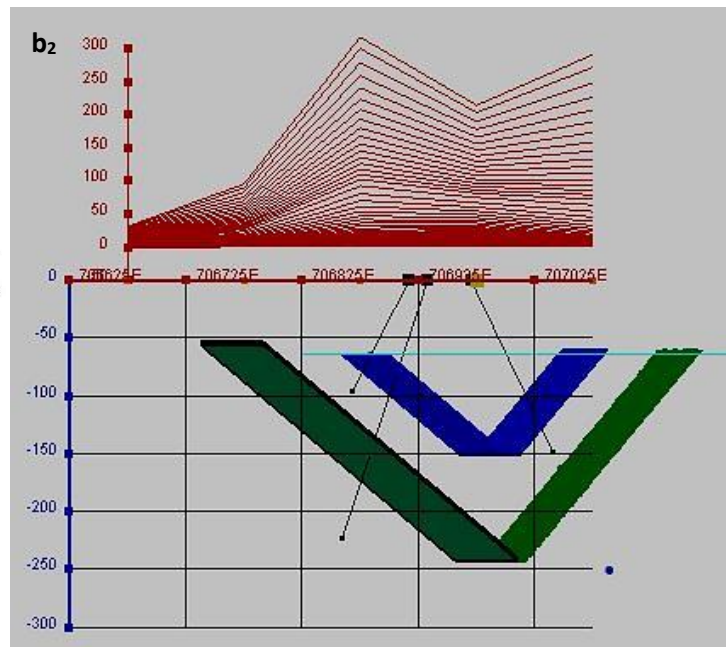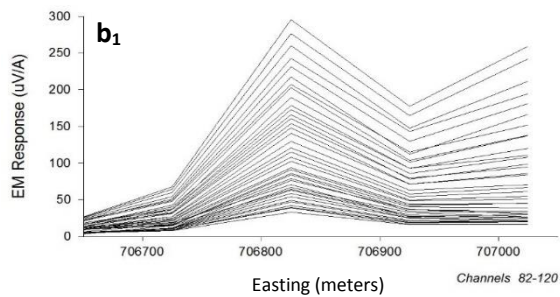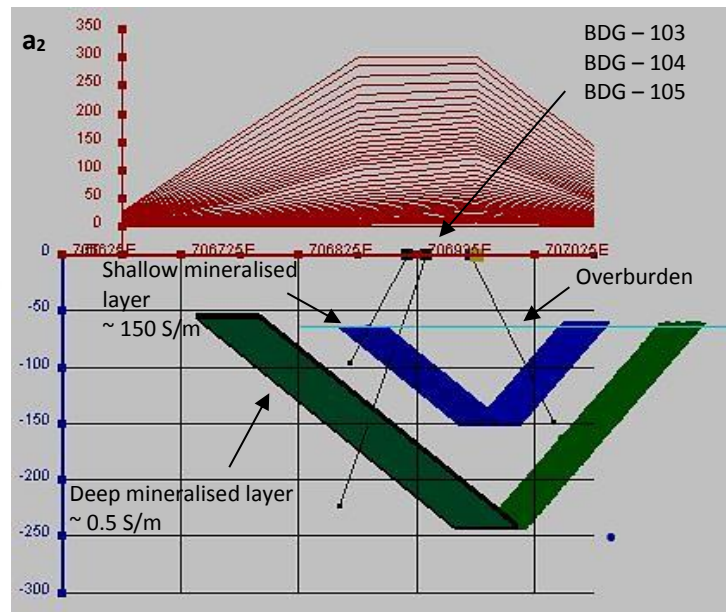
4.2 GURUBANG DEPOSIT

Ground-based TDEM modelling

EM modelling has more variables than magnetics or gravity. The signal amplitude at any given time-channel is a complex function of size, orientation, conductance, location and depth. Simplistically, high amplitude signals could indicate the presence of a small, highly conductive response, but it could also suggest a large, weak conductor. On the other hand, low amplitude signals could suggest either a poor or strong conductor at great depth, or possibly a good conductor at a shallow depth that is poorly coupled with the Tx loops. To overcome this ambiguity, a forward modelling approach was utilised. The EM models in this section best fit the TDEM datasets collected across the Gurubang deposit area. Profile 390N was not subject to modelling because of the overabundance of surficial noise.

Profile 590N

A confined sheet model, shown in Figure 14 a_2, best fits the observed TDEM data for profile 590N (Figure 14 a_1). The model is based on a multi-layered geometric structure that incorporates a relative thick (50 – 60 m) overburden layer and two mineralised horizons, at varying depths. The depth to the mineralised layers were based on the drill core logs from the available exploration reports (Table 1 in Chapter 2). The shallow mineral zone was intercepted by three of the drill cores (BDG – 103, 104 and 105). A second deeper mineralised zone was intercepted by drillcore BDG – 105. Conductivity measurements were acquired for the shallow layer and showed a range between 150 – 250 S/m. Unfortunately, no conductivities were measured for the deeper layer.

Compiled geological interpretations were useful in constraining the strike azimuth and dip orientation of the layered plates. The eastern limb of the deposit shows an approximate dip 50°
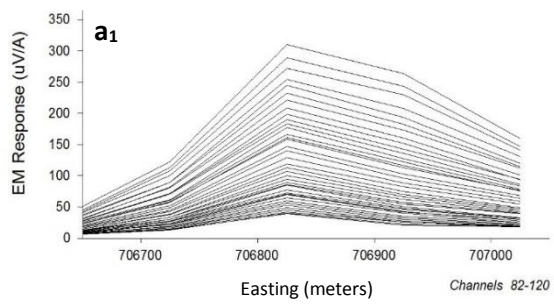
(Figure 14. TDEM profiles and forward models across the Gurubang deposit locality. a_1. Profile 590N a_2. Model profile 590N b_1. Profile 490N b_2. Model profile 490N c_1. Profile 290N c_2 Model profile 290N. Location of intersected drill holes is shown. v = h)

towards the west, while the western limb was given an approximate dip of 45° to the east. The shallow mineralised horizon was given a conductivity value of approximately 150 S/m, which gave a reasonable match to the observed data. As no petrophysical measurements were taken of the deeper layer, the data was analysed using a range of conductivity values and a value of 0.5 S/m gave the most reasonable fit to the data.

Profile 490N

Extending the strike length of the two-sheet structure used to fit the data in profile 590N to beneath profile 490N, gave a reasonable fit to the shape and amplitude of the obtained data (Figure 14 b_2). Geometrically, the model aligned with a multi-layer structure, with mineralisation at depths constrained by the intersecting drill cores. The best fit to the data was achieved using strike lengths ranging from 150 - 170 m for the shallow layer and $160 - 180$ m for the deeper layer. Both mineral layers terminate at profile 390N.

Profile 390N

-   No analysis performed due to high noise contamination (stated previously).

Profile 290N

A single confined sheet model (Figure 14 c_2), gives a reasonable fit to the mid- to late-channel time response in the eastern section of profile 290N (Figure 14 c_1). The depth extent, dip, dip direction, strike azimuth and conductivity were constrained via information from the intercepting drill core (BDG $- 102$). The plate extends to a depth of 70 m, has a dip of 50° towards the west, trends 340° NNW-SSE and was given a conductivity of around 250 S/m.

Ground-based magnetic modelling

The general geometric structure of the mineral deposit, based on the TDEM model, in conjunction with previous drill hole interpretations, was then integrated into the magnetic modelling. The aim being to evaluate how significant the magnetic response associated with the mineralisation is on the overall observed magnetic signature and whether the data assists in constraining the model parameters. Average magnetic susceptibility values (Table 1 in chapter 2), were used to constrain the magnetisation of the two mineralised layers. As magnetic susceptibility was not measured for the host rock sections of the extracted drill cores, susceptibilities were based on the values collected from the rock samples during the preliminary trip (Table 2 in chapter 2) and from the susceptibility ranges provided by Dentith and Mudge (2014). Based on the collected host rock susceptibilities, the host

rock is assumed to be relatively non-magnetic, which was a factor taken into consideration when developing the models.

The two-layered mineral model (Figure 15) gave a poor fit to the magnetic data obtained from the northern section of the Gurubang area because according to the previous exploration reports, the average susceptibility of the two mineralised horizons range from $0.03 - 0.05$ SI (Table 1 in chapter 2). Values within this range were trialled but did not achieve a good match to the data. Doubling the magnetisation of the layers provides a better match to the data intensity. However, the general shape of the modelled response was a poor fit to the data.

The depth to top of the body and thickness of the mineralisation was constrained using the intersecting drill logs. The thickness of the shallow horizon ranges from $5 - 15$ m, while the deeper layer ranges from $40 - 50$ m. The western limb of the mineralised layers was given an approximate dip of 50° E, while the eastern limbs have a steeper dip of about 60° W. These dips were based on the strikes and dips presented in the previous geological interpretation (Castle, 1976). Dip orientation ranges from $330^{o} - 340^{o}$ NNW-SSE, which matches the overall orientation of the geological framework (Castle, 1976). The strike length of each mineralised layer was constrained via the TDEM model. The strike length of the shallow horizon was around 160 m, while the deeper layer has an approximate strike length of 170 m.
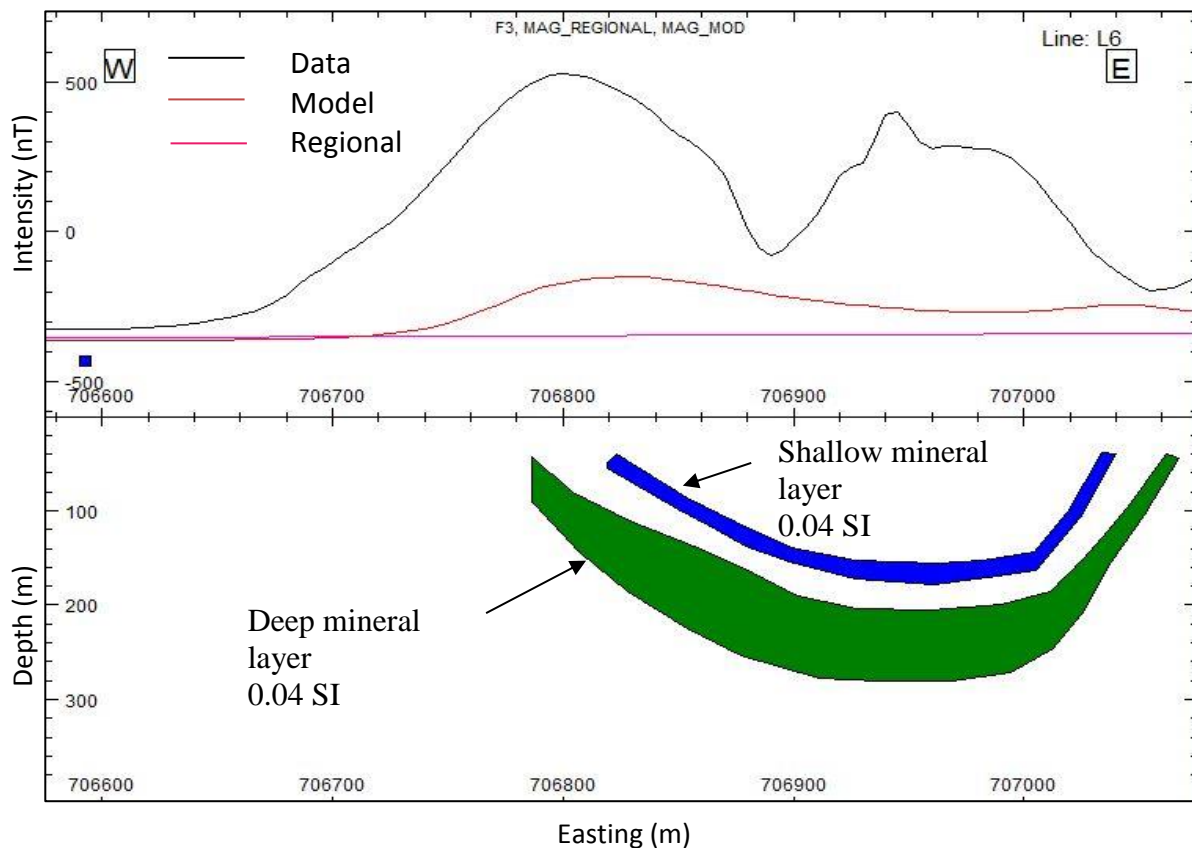
(Figure 15. Magnetic model seen from line 6, of the two mineralised layers that constitute the northern section of the Gurubang area.)

Unable to achieve a reasonable fit to the observed magnetic data using only the mineralisation, suggests that there are other sources contributing to the overall magnetic response. A variety of scenarios incorporating different body shapes and parameters were then trialled and tested against the collected data. Due to non-unique solutions to the modelling, two possible solutions are presented below.
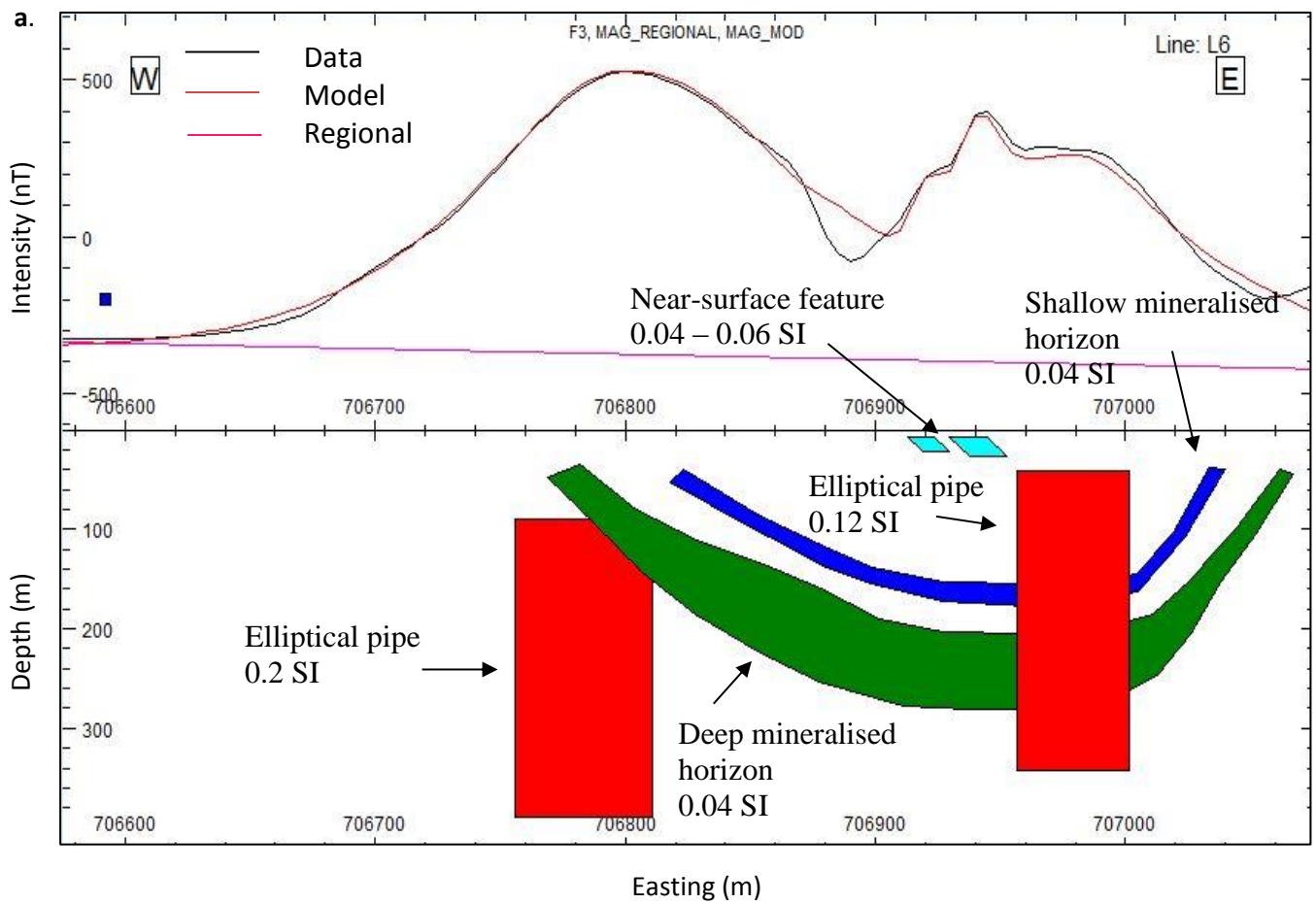
Scenario 1

Additional geological bodies were integrated into the mineralised model (Figure 16 a and b), which gave a reasonable fit to the observed data. A vertical elliptical-pipe body was then used to match the broad magnetic response seen in the northwest section of the survey area. The body is found at a depth of approximately 90 m and has a magnetic susceptibility of 0.2 SI. Regarding the body's geometry, it has a width of about 60 m and strikes nearly 80 m north-south. Although the body is shown with a vertical dip, it can be modelled with dips ranging from $80^{\circ} - 110^{\circ}$. A second vertical elliptical pipe was used to model the eastern broad magnetic response. The body was given a magnetisation of 0.12 SI and is found at a depth of approximately 45 m. The body strikes north-south for about 40 m and was given a width of around 25 m. Near-surface tabular bodies, given susceptibilities ranging from $0.04 - 0.06$ SI, provided a reasonable match to the high frequency signals. The bodies are found at a depth of around $10 - 15$ m and have a width of around 10 m.

Scenario 2

The magnetic model in scenario 2 (Figure 17 a and b), gives a reasonable fit to the magnetics data. This was achieved via the following: replacing the eastern pipe (scenario 1) with a magnetic (0.12 SI) near-surface layer; altering the geometry of the western pipe body, and by lowering the magnetic susceptibility of the western section of the deep mineralised layer.

The geometry of the near-surface layer involves a strike of approximately 20 m north-south, a width of around 60 m and a depth extent of 35 m. The feature is situated at a depth ranging from 40 – 50 m and cross-cuts the drill core BDG-103 at an approximate depth of 50 m. The elliptical pipe-body achieves a reasonable match to the western magnetic anomaly. The pipe was given a width of approximately 40 m, strike length of 80 m and a magnetic susceptibility of around 0.2 SI. To successfully model the central magnetic low, a portion of the deeper mineralised zone was given a lower magnetic susceptibility (0.06 SI). Also, the shape of the portion was slightly altered to best fit the data. The two near-surface features with susceptibilities ranging from $0.04 - 0.06$ SI were incorporated into the model. The features are found between $5 - 10$ m depth and have a width ranging from $5 - 20$ m.
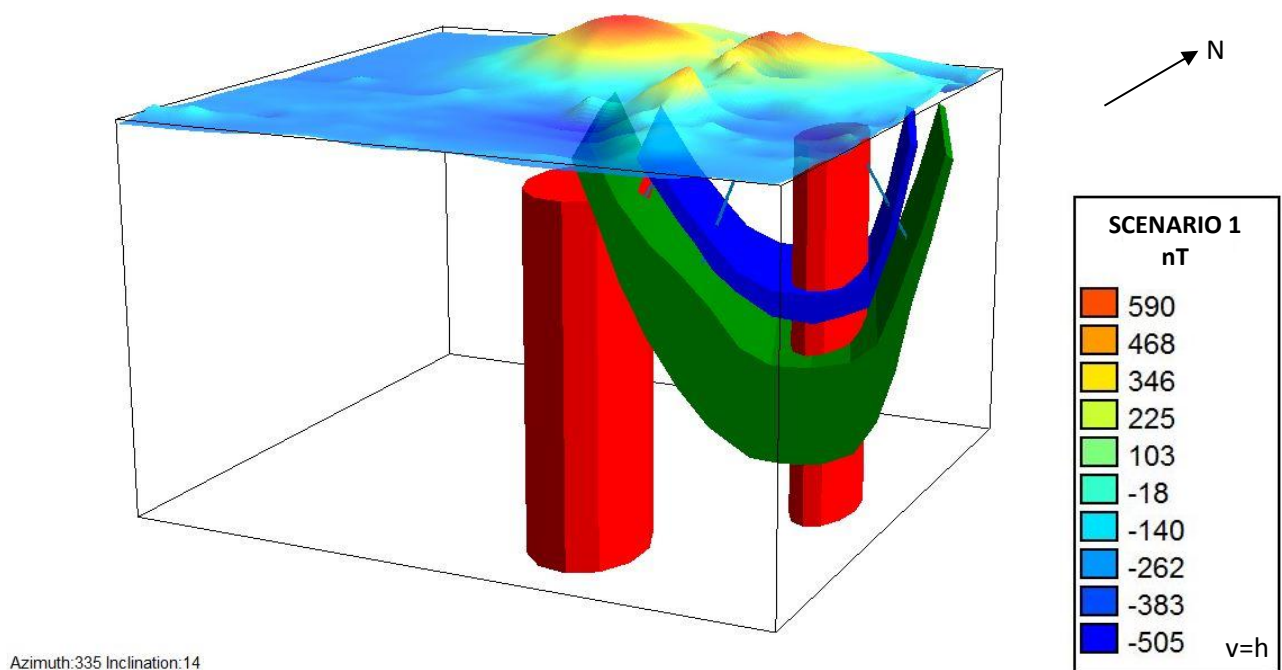
(Figure 16. Scenario 1 magnetic model associated with the mineralisation.
a. Line 6 x-section outlining the two-layered model with additional bodies.
b. 3D perspective of layered mineralisation sulphide deposit with additional geological
features.)

a.

Near-surface features
0.04 - 0.06 SI

Shallow mineralised
horizon
0.04 SI

Near-surface
layer
0.12 SI

Elliptical pipe
0.2 SI

Altered deep
mineralised section
0.06 SI

Deep mineralised
horizon
0.04 SI

b.

SCENARIO 2
nT

590
468
346
225
103
-18
-140
-262
-383
-505

v=h

Azimuth:342 Inclination:11
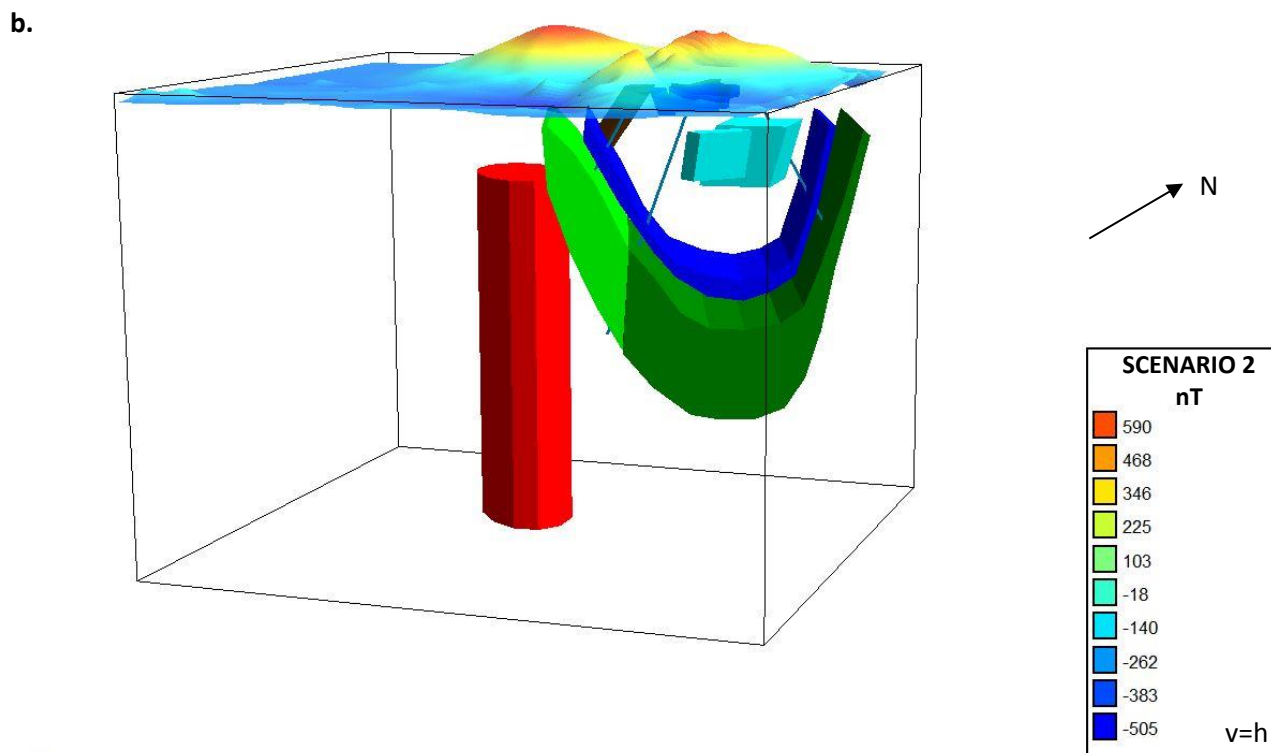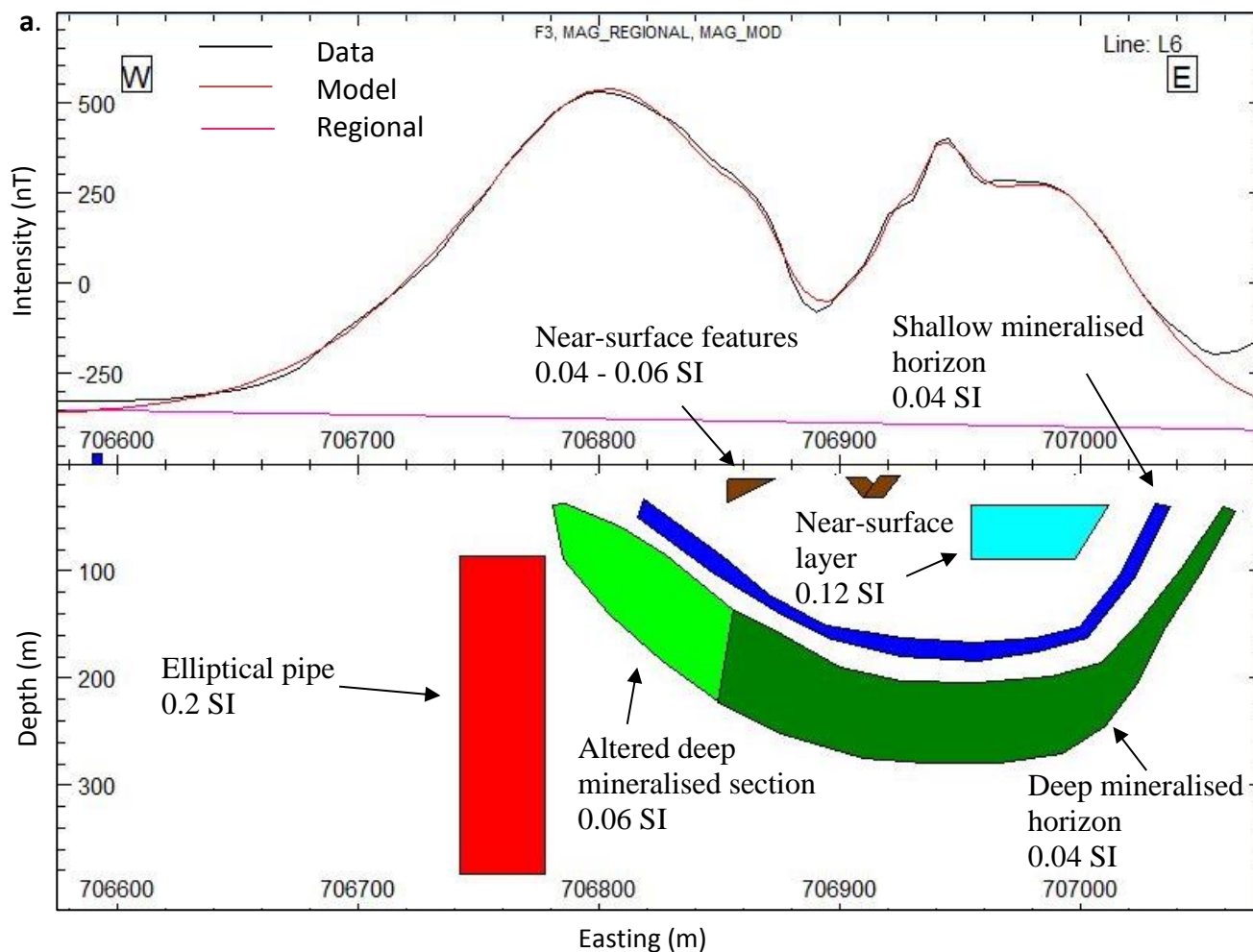
(**Figure 17. Scenario 2 magnetic model associated with the mineralisation.**
a. Line 6 x-section outlining the two-layered model with additional bodies.
b. 3D perspective of layered mineralisation sulphide deposit with additional geological
features.)

A single mineralised layer model gives a poor fit to the magnetic data obtained in the southern section of the Gurubang survey area. The model was based on the TDEM model of the conductive response in the eastern section of profile 290N. The magnetic susceptibility of the mineralised layer was constrained using the measured susceptibilities from the previous drill logs (Cooke, 1977). Susceptibilities ranging from 0.03 – 0.05 SI were trialled but were unable to explain the broader magnetic signatures. The layer was given a dip of approximately 50° towards the west, strike length of around 150 m, width of 4 m and a depth extent of 40 m.

A reasonable fit to the data was achieved by incorporating additional bodies into the single mineralised layer model (Figure 18). These bodies included two near-surface layers and two near-surface features. The magnetic susceptibility of the near surface layers ranged from 0.02 – 0.05 SI. The layers were given a strike length of around 100 m and range in width from 20 – 40 m. Both near-surface layers have a dip of around 50° towards the east and a depth extent of 25 m. The two near-surface features are located at a depth of 5 – 10 m and were given a magnetic susceptibility of around 0.01 SI. The width of the bodies ranges from 5 – 10 m.
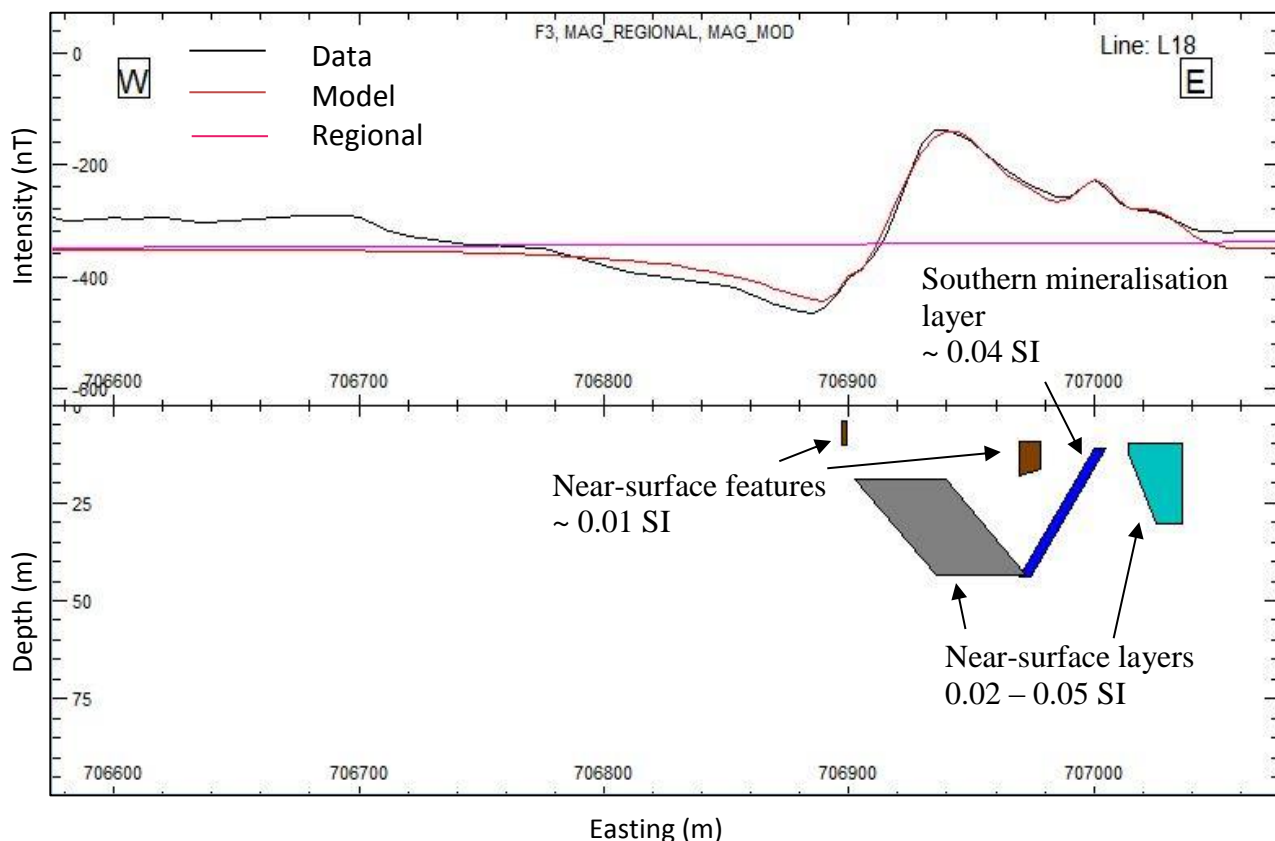

(Figure 18. Computational model seen from line 18, of the single mineralised layer that was intersected in the southern section of the Gurubang area.)

Ground-based gravity modelling

Two computational gravity models, model 1 and 2, were generated to explain the gravity response obtained across the Gurubang mineral horizon. The previously acquired drill core density measurements (Table 1 in chapter 2), in conjunction with the values from the collected preliminary rock samples (Table 2 in chapter 2), were used to constrain the densities of the mineralised layers and surrounding host geology. However, due to lack of outcrop in the area, the density values of the collected rock samples may not be representative of the overall lithology.

Model 1

A reasonable fit to the gravity data was achieved using two adjacent geological units with contrasting density values (Figure 19). The limestone unit has a density susceptibility of 2.56 g/cm^3, while the contrasting undifferentiated unit has a density of 2.8 g/cm^3. The width of each unit is based on the outcropping geological interpretation by Cooke (1977). The limestone unit was given a width of approximately 200 m, while the adjacent undifferentiated sediments was given a width of around 220 m. All units strike for approximately 1000 m. The background geology was given a density value ranging from 2.6 – 2.7 g/cm^3, which was based on providing the best match to the data.
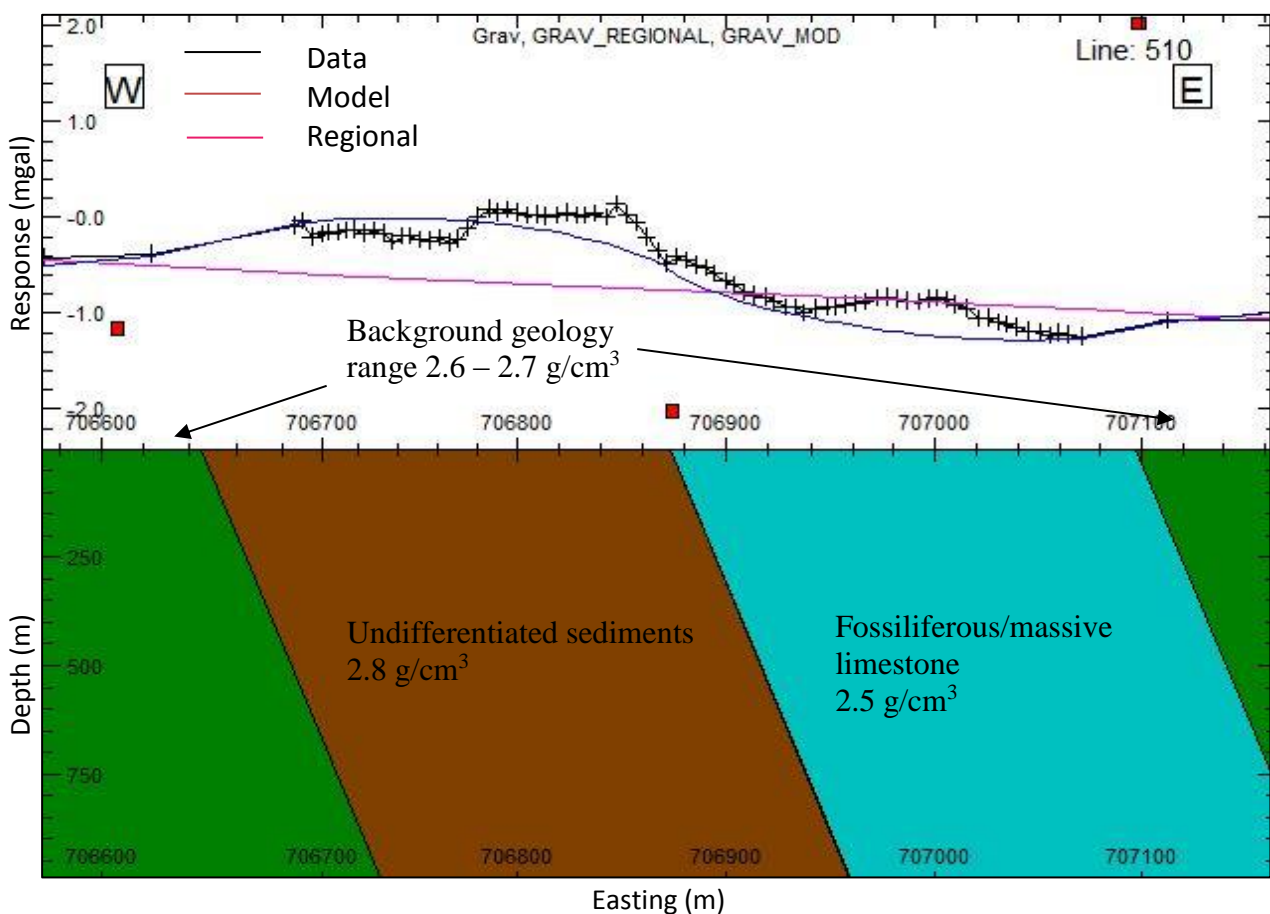
(Figure 19. Bouguer anomaly gravity response showing the major geological units comprising the Gurubang site.)

Model 2

Model 2 (Figure 20) integrates the mineralised magnetics model (Model 1) into gravity model 1, which gives a moderate fit to the observed data. Density values were constrained using the measured values of the drill cores. The most reasonable fit to the data was achieved using values between $3.5 - 3.8$ g/cm^3 for the mineralised zone and a density between $2.9 - 3.0$ g/cm^3 for the vertical pipe.
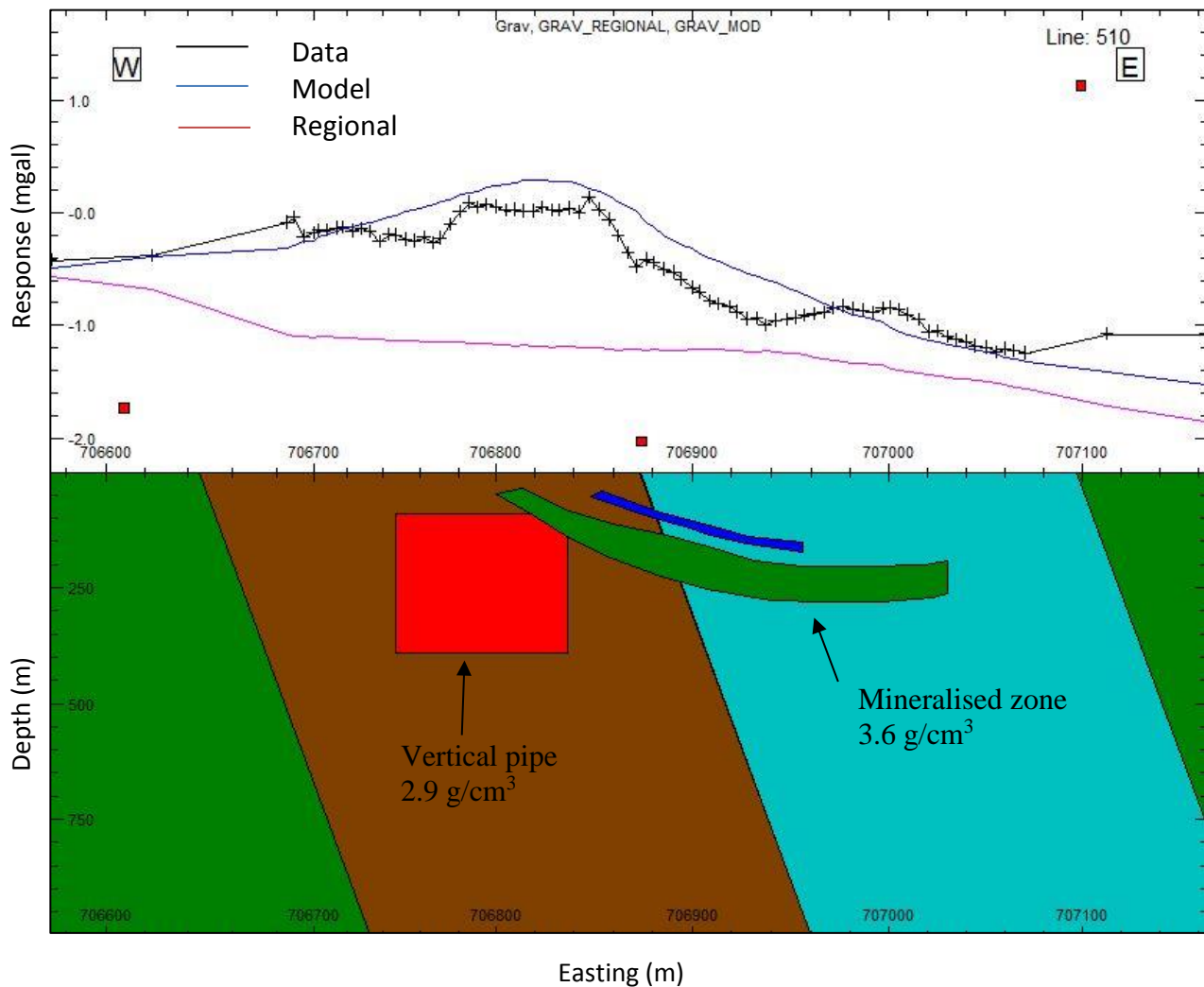
(Figure 20. Bouguer anomaly gravity response incorporating the background geologies from model 1, mineralization zone and vertical body from the magnetics model 2.)

4.3 ROSEBANK DEPOSIT

Ground-based TDEM modelling

Modelling the TDEM dataset collected across the Rosebank deposit was purely conceptual as there was inadequate geological information to constrain the potential deposit. Various sheet models were trialled and tested, providing acceptable ranges for each parameter. Drill log data helped constrain various parameters for the eastern section of the survey area (Table 1 in chapter 2).
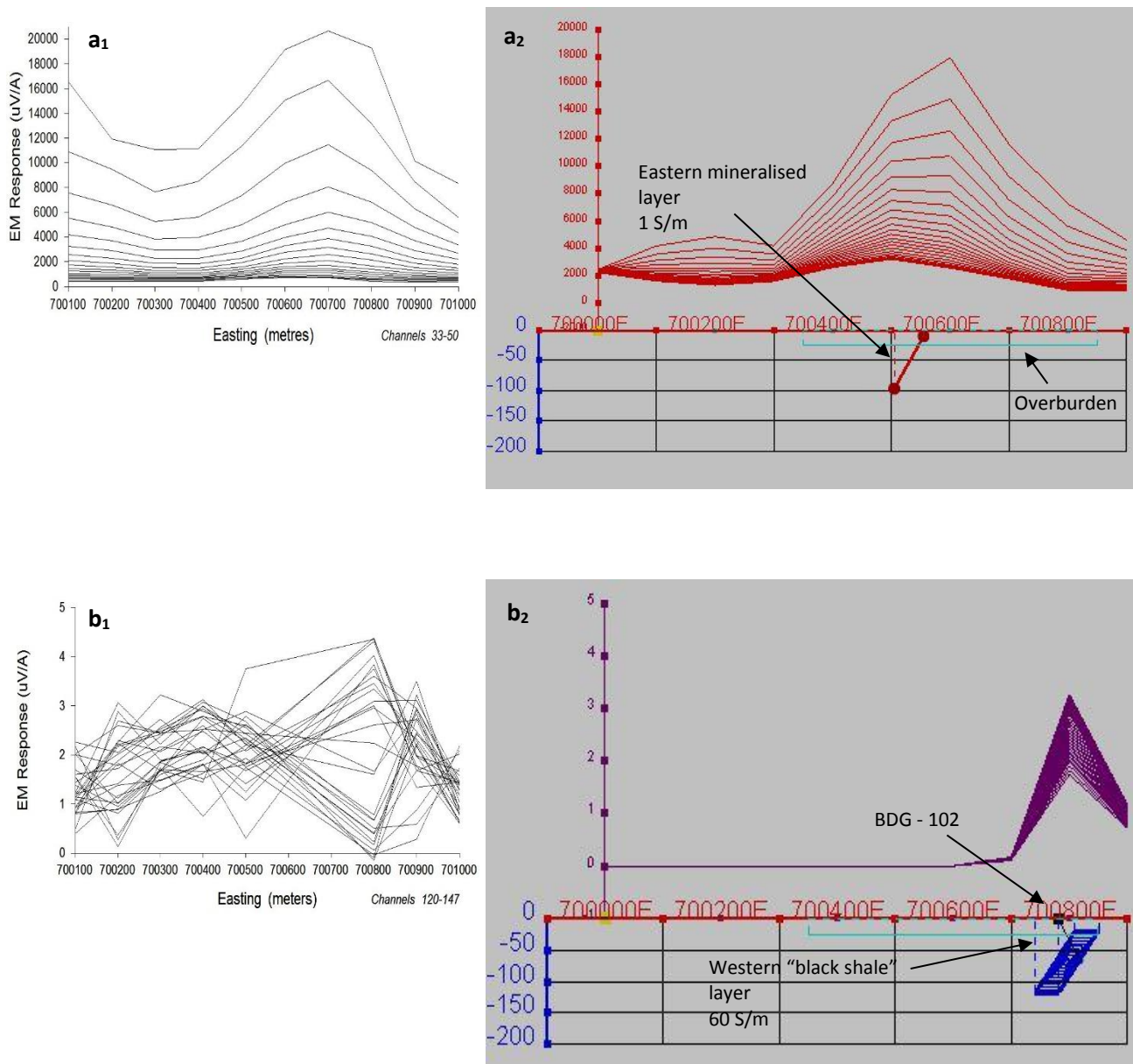
(Figure 21. TDEM profiles and forward models across the Rosebank deposit locality.
a1. Profile 250N; a2. Model Profile 250N
b1. Profile 350N; b2. Model Profile 350N.
Location of intersecting drill hole is shown. v = h)

Profile 250N

A single sheet model (Figure 21 a_2) gave a reasonable fit to the mid-channel time response (Figure 21 a_1) along profile 250N and 350N. The potential body is found at a depth of 43 m, dipping 52° towards the west. The dip was constrained via the geological interpretation provided in the previous mapping reports (Rabone, 1978). Trialled conductivity values were based on the accepted ranges provided by Dentith and Mudge (2014). The achieved model uses a conductivity of 1 S/m.

Profile 350N

An additional sheet (Figure 21 b_2) was incorporated into the model to explain the late-channel time response (Figure 21 b_1). Body parameters were constrained via previous geological interpretations and drill log (Rabone, 1978)). The body is situated at a depth of 20 m and dips 55° towards the west, which conforms with the apparent dip of the overall geology. Also, the body has a strike of 420 m, and trends about 350° NNW-SSE. Conductivity was set to 60 S/m and was based on the value ranges set by Dentith and Mudge (2014).

Ground-based magnetics modelling

The geometric structure of the two TDEM models were incorporated into the magnetics data (Figure 22). Magnetic susceptibility of the two individual bodies was constrained using appropriate susceptibility ranges provided by Dentith and Mudge (2014). The western body was given an approximate dip of 50° towards the west, a thickness of around 20 m and a susceptibility of 0.004 SI. This was the susceptibility that best matched the intensity of the magnetic signature. The eastern tabular body was given a magnetic susceptibility of 0.004 SI and a thickness of 15 m, which gives a reasonable match to the magnetic response. The two structures were given an azimuth orientation of 350° NNW-SSE, based on the trend of the host geology and TDEM model.
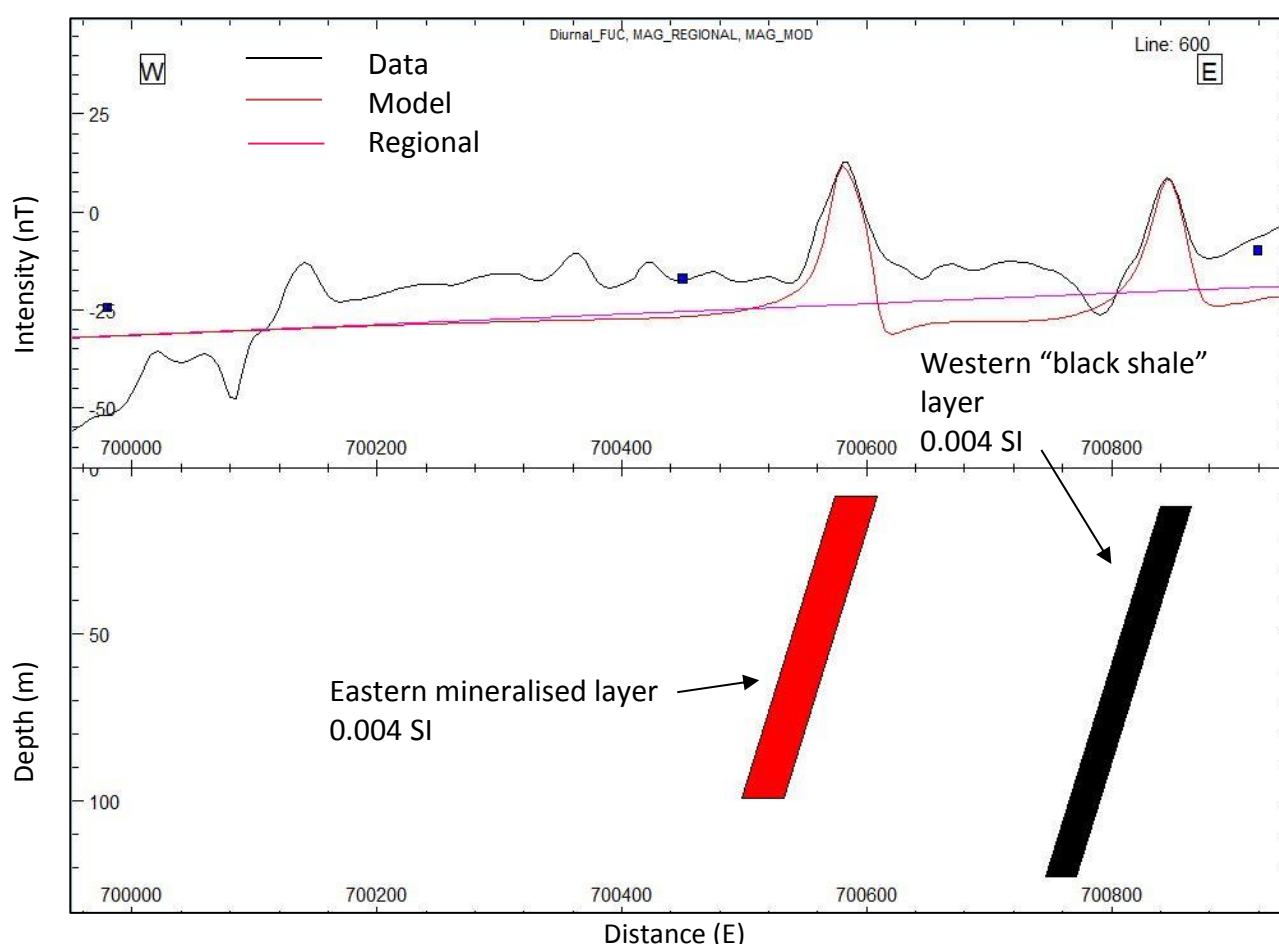
(Figure 22. Computational magnetic model associated with the Rosebank mineralisation. x-section outlining the two-layered model seen along line 600N.)

Ground-based gravity modelling

Two models (Figure 23 a and b) were generated using the high-resolution, ground-based gravity corrected data obtained across the Rosebank deposit site. Density values given to each unit was constrained using a combination of accepted ranges provided by Dentith and Mudge (2014) and best matching the data response.

Model 1

Model 1 (Figure 23 a) incorporates 3 tabular bodies, representative of the contrasting host geology. All bodies dip 60° east and have a strike length of approximately 100 m striking 350° NNE-SSW. The western most unit was given a density of 2.67 g/cm³ and a width of 250 m. The central unit has a width of 145 m and was given a density value of 2.52 g/cm³. The eastern unit has a width of approximately 500 m and was given a density of 2.67 g/cm³. The unit width based on previous geological mapping (Cooke, 1977) and providing the best match to the data response.

Model 2

Model 2 (Figure 23 b) incorporates both the host geology from model 1, and the tabular bodies based on the magnetics model (Figure 22). A variety of density measurements, based on ranges set by Dentith and Mudge (2014), were trialled for the mineralised units. The eastern "black shale" mineralised unit was given a density ranging from 2.26 g/cm^3, to match the data response. The western unit was given a density ranging for 2.67 - 2.9 g/cm^3.
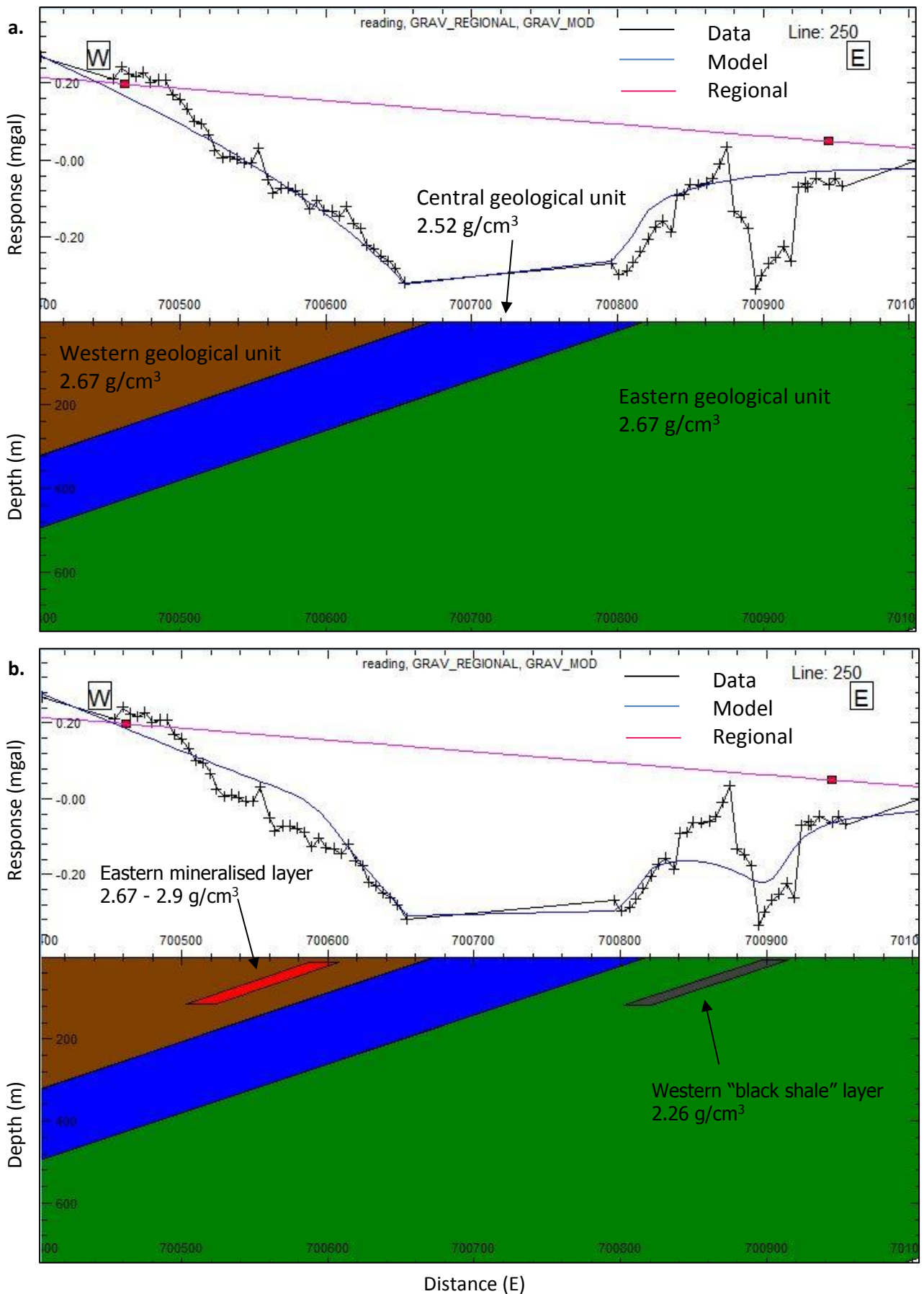
(Figure 23. a and b are bouguer anomaly profiles associated with the Rosebank deposit area.
a. Gravity model incorporating geological framework.
b. Gravity model of the geological framework and additional mineralized zones.)

CHAPTER 5

INTERPRETATION AND DISCUSSION OF GEOPHYSICAL SIGNATURES OF SMALL-SCALE BASE METAL DEPOSITS

5.1 INTRODUCTION

This chapter aims to interpret and discuss the high-resolution geophysical data and computational models related to the target small-scale base metal deposits. This analysis will highlight the geophysical methods most useful in delineating and evaluating the mineralisation, and present new information regarding the geological framework of the two deposit localities.

5.2 DETECTION AND EVALUATION OF TARGET SMALL-SCALE BASE METAL DEPOSITS
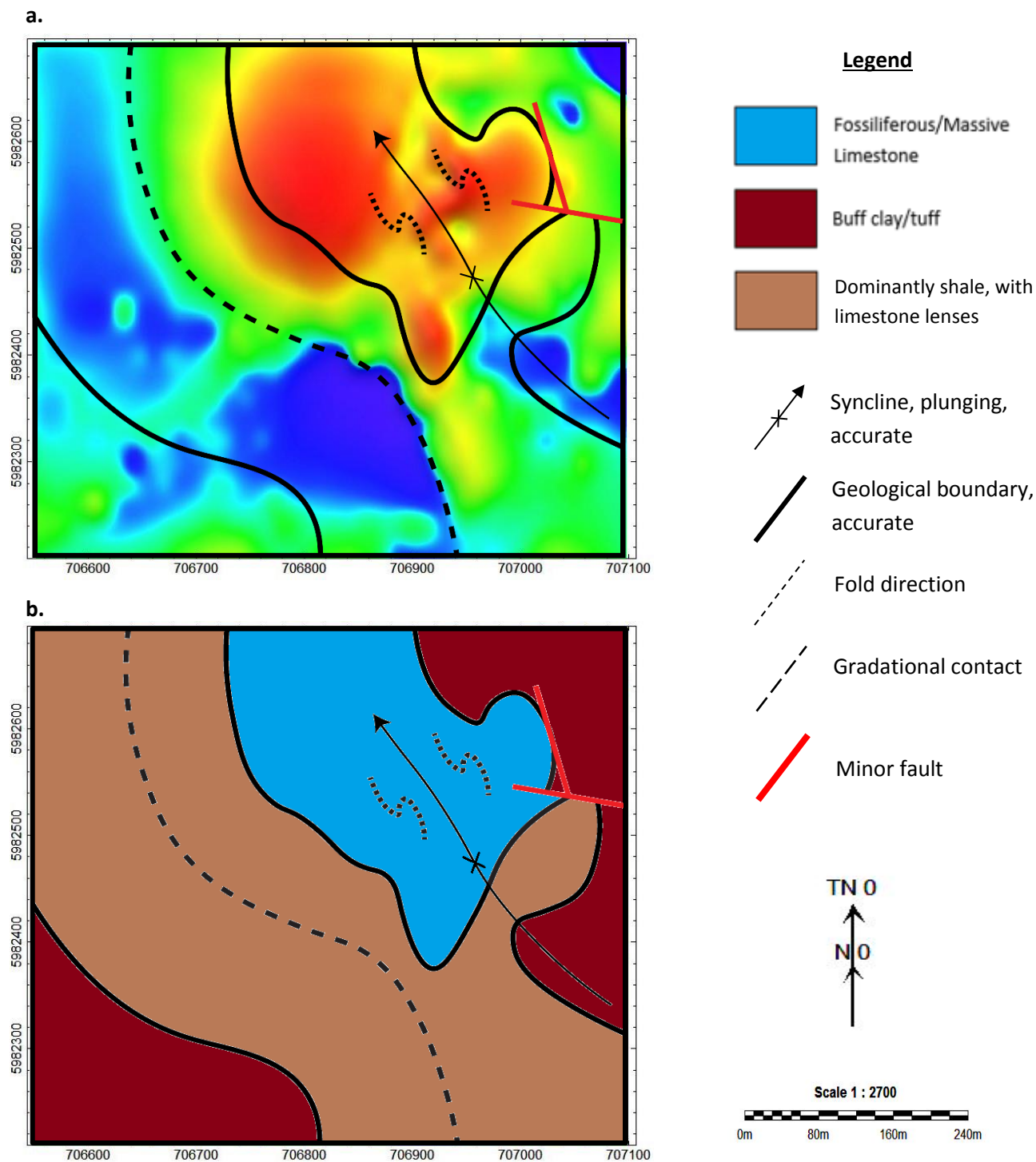
Gurubang deposit

The data presented in chapter 3, shows the geophysical response associated with the Gurubang VHMS base metal deposit. The mineralisation itself gives rise to the TDEM response due to its content of conductive sulphide (mainly pyrrhotite) minerals, as noted in the petrophysical study of previously acquired core sample (Table 1 in chapter 2). Successful TDEM modelling (Figure 14 in chapter 4) indicates that the mineralisation occurs within two distinct layers. These include a shallow relatively thin layer and a deep thick layer. According to previous geochemical studies of the collected drill cores, the shallow relatively thin (5 – 10 m) layer represents a semi massive "ore equivalent" pyrrhotite-rich horizon, while the deeper layer represents a thick (40 – 50 m) horizon of massive sulphide material (Table 1 in chapter 2). The model layers appear to dip towards one another creating a synform, which agrees with the previous geological interpretation of the Gurubang area (Castle 1976; Argaud, 1976, and Cooke, 1977). The data can be modelled using a dip ranging between 45° – 60° for the western limb and 55° – 70° for the eastern limb, suggesting an open to close synform fold. This style of mineralisation is in support of the idealised volcanogenic massive sulphide Gurubang model put forward by Gunn and Dentith (1997).

TDEM in conjunction with the magnetic (Figure 17 in chapter 4) and petrophysical data (Table 1 in chapter 2), indicates a shallow mineralisation horizon that extends towards the south eastern section of the surveyed area. The section of mineralisation is relatively thin (2 – 5 m), with a strike length of around 100 m and dips around 50° towards the west, which conforms to the relatively dip of the eastern portion of the mineralisation to the north. This suggests that the overall

mineralisation has a total strike length of approximately 400 – 450 m and may extend beyond the boundaries of the survey area.

The relatively intense magnetic signature (Magnetic Anomaly Map, Figure 24) associated with the Gurubang deposit is primarily generated by its iron sulphide-rich mineralogy. According to Castle, 1976 and Cooke, 1977, the deposit contains high concentration of iron-sulphide minerals including pyrrhotite, which in high concentrations produces a contrasting magnetic signature to the host rock (Dentith and Mudge, 2014). The magnetic models (Scenario 1 and 2) depicted in chapter 4, suggest that the mineralogy cannot solely explain the two broader magnetic signatures seen in the north. As such, two intrusive bodies were integrated into the first model (Scenario 1, Figure 16 in chapter 4) providing a more reasonable fit to the observed data. Although the intrusive bodies appear vertical in the models, variations in dip ($\pm$ 30°) also produce a reasonable fit to the data. The first magnetic model was nullified because trialling a sub-sectioned mineral deposit gives a poor fit to the TDEM data. As a result, a second model (Scenario 2, Figure 17 in chapter 4) was developed, providing a reasonable fit to the data. The model incorporates a vertical pipe body located in the north west and numerous magnetic near-surface features located in the north east. The vertical pipe may be representative of an intrusive Tertiary basaltic volcanic plug, which are known to occur within the immediate region (McQueen, 1994). The high frequency signals in the north east were successfully modelled using numerous near-surface features of varying susceptibilities, shapes and sizes. The apparent dips of the near surface features were based on achieving the best fit to the data. Potential causes of the high-frequency signals include a Tertiary basalt cover unit (Glen and Lewis, 1994), an intermittent dyke intrusion, or possibly outcropping gossanous material containing maghemite leached from the deeper mineralisation (Cooke, 1977).

The high-resolution gravity data (Figure 13 in chapter 3) highlights different geological structures with contrasting density values. According to the gravity models (Figure 19 and 20 in chapter 4) the prospective host geology is the primary cause of the overall contrasting gravity response across the target area. By comparing the gravity response to the magnetic data, there is a distinct correlation across the broad magnetic feature located in the north west (Figure 8 a and c in chapter 3). Forward modelling the gravity response utilising the magnetic structures proved challenging. By altering the densities of the mineralised horizons and proposed vertical intrusive pipe, a reasonable fit to data was achieved. These densities are based on providing the best fit to the acquired data and fall within the mineral susceptibility ranges provided by Dentith and Mudge (2014).

a.

b.

**(Figure 24. a. Gurubang magnetic anomaly map with geological interpretation overlaid.
b. Simplified diagram of interpreted geological units.
Geological interpretation modified from Cooke, 1977.)**

Legend

Fossiliferous/Massive Limestone

Buff clay/tuff

Dominantly shale, with limestone lenses

Syncline, plunging, accurate

Geological boundary, accurate

Fold direction

Gradational contact

Minor fault
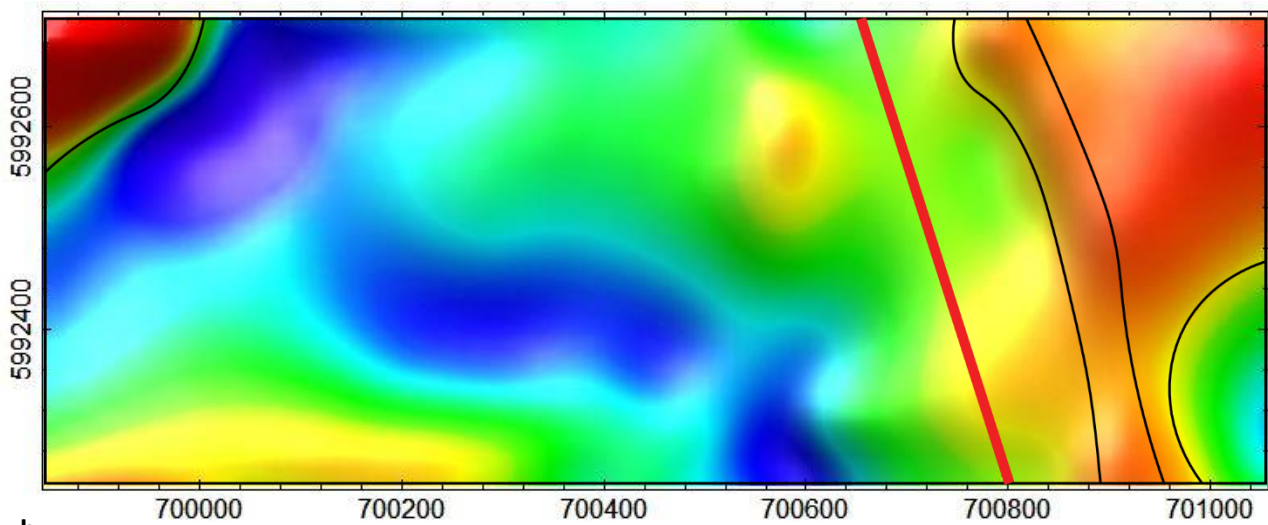
TN 0

N 0

Scale 1 : 2700

0m   80m   160m   240m

Rosebank deposit

Data presented in the second section of chapter 3, displays the geophysical response associated with the Rosebank deposit area. The TDEM response suspected to be related to the mineral horizon is caused by the abundance of conductive, pyrite-pyrrhotite material. Without direct drill sampling of the Rosebank deposit, trialled forward models are primarily based on previous geological interpretations of surface indicators and physical property ranges provided by Dentith and Mudge (2014). TDEM modelling indicates a single mineralised layer within proximity of the old abandoned mine shaft (Nagy, 1977). The mineral layer appears to have a relative dip of~ 50° towards the west and strikes 340° – 350° NNW-SSE, which conforms to the known structural habit of the host stratigraphy (Castle 1976; Argaud, 1976, and Cooke, 1977). This suggests that the mineralised layer is structurally bound. Also, the TDEM survey identified the black "graphitic" shale located in the eastern section of the deposit area. This anomaly was intersected during a prior drilling expedition (PH – 1), which provided constraints for modelling parameters. The graphitic shale appears to have a dip of approximately 50° towards the west with a conductive response that falls in the range of graphitic shales, as referred by Denith and Mudge (2014). According to the TDEM models, the strike length of both mineralised layers ranged from $50 – 60$ m. However, data limitation confines the strike length to the surveyed area.
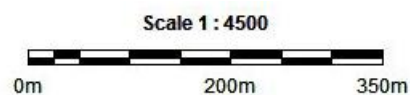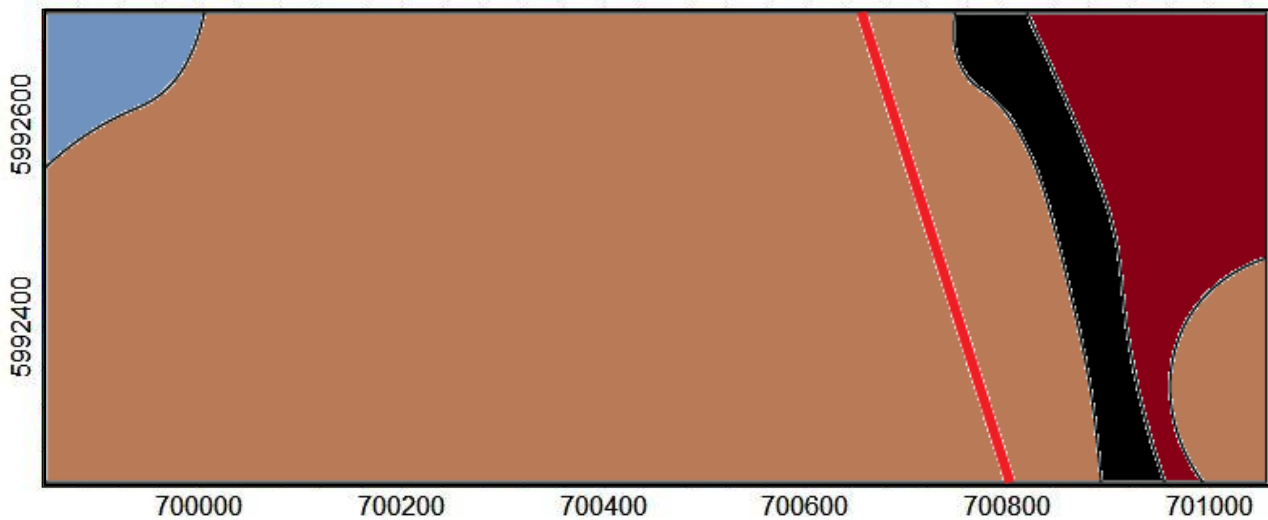
The magnetic response related to the two anomalies identified via the TDEM data (Figure 22 in chapter 4), show similar magnetic intensities. According to the petrophysical study of the black shale, the unit contains around $5 – 25\%$ pyrite ($\pm$ pyrrhotite). The pyrrhotite present within the layer would be the primary cause of the contrasting magnetic response (Figure 25). The black shale was modelled using the readily available petrophysical information obtained from the percussion fragment samples (Table 1 and 2 in chapter 2). The model shows a relatively thin stratiform magnetic layer, dipping about 50° towards the west. As for the potential Rosebank mineralised layer, the magnetic susceptibility and body thickness was based on matching the wavelength and intensity of the observed magnetic anomaly. The resulting magnetisation is almost identical to that of the magnetisation of the black shale, potentially suggesting that the Rosebank deposit is hosted within a western lens of the black shale unit (Figure 25 b). This supports the original claim by Herzberger and Barnes (1978), that the mineral deposit is hosted in a sedimentary shale unit, as seen in Figure 25.

The gravity data (Figure 13 in chapter 3) associated with the Rosebank site, highlights areas of contrasting densities. The previously drilled black 'graphitic' shale (Table 1 in chapter 2) appears less dense than its host stratigraphy, possibly related to the leaching of dense material into the surrounding host rock via hydrothermal fluids. These fluids may have been driven by the initiation

a.

b.

Scale 1 : 4500

0m   200m   350m

Legend

(brown)	Dominantly shale – dark green, sandy interbeds
(blue)	Basalt capping
(dark red)	Tuff – course grained, interbedded chert
(black)	Black 'graphitic' shale horizon

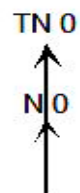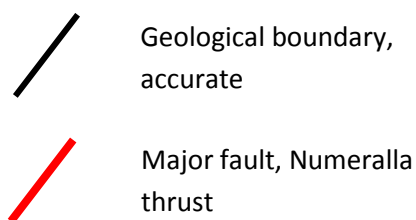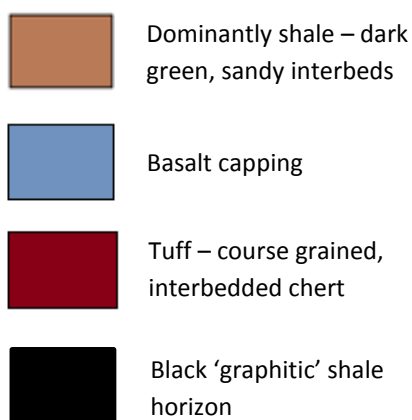Geological boundary, accurate

Major fault, Numeralla thrust

TN 0

N 0

(Figure 25. a. Rosebank magnetic anomaly map with geological interpretation overlaid.
b. Simplified diagram of interpreted geological units.
Geological interpretation modified from Nagy, 1977.)

of the Numeralla fault (directly adjacent to the shale). The density value that best matches the gravity data (Figure 23 b in chapter 4), falls within the acceptable range for graphitic shale, as described by Dentith and Mudge (2014). As for the western anomaly, there is no clear contrast in gravity response between the potential mineralisation and the host rock. This may be due to the quantity of dense material being too small to be identified via a gravity survey of this resolution.

The high-resolution gravity survey was very effective in identifying the Numeralla fault (Nagy, 1977). The fault is associated with a low gravity response compared to the surrounding geologies. This suggests that a high-resolution gravity survey is useful in delineating crustal features such as major fault structures.

5.3 GEOPHYSICAL SIGNATURES RELATED TO GEOLOGICAL FRAMEWORK

Gurubang deposit area

The Gurubang deposit is hosted in a mid-late Silurian sequence of rock composed of shallow marine sediments and felsic volcanic rocks (Cooke, 1977). The TDEM data, although not typically used to examine the local geological framework, supports the idea of an open to close synform (Figure 26). This structure supports the previous geological interpretations of the Gurubang field site (Cooke, 1977). Also, the TDEM data indicates that the mineralisation conforms to the general strike orientation of the regional geology (NNE-SSE).

The high-resolution magnetic and gravity surveys effectively highlight the primary anomaly complex of interest, as well as deeper basement features (Figure 24 a and b). The primary anomaly complex constitutes a mixture of altered shallow marine sediments, relatively large intrusive pipe and the mineralised horizons (Figure 25). The basement geology has a lower magnetic signature relative to the proposed mineralised area (Cooke, 1977), and appears to strike 330o − 340o NNW–SSE. Features, such as the near-surface anomalies, have strike orientations similar to that of the proposed folding direction, suggesting emplacement was prior to most recent folding event at around 400 − 380 Ma (Foster and Gray, 2000).
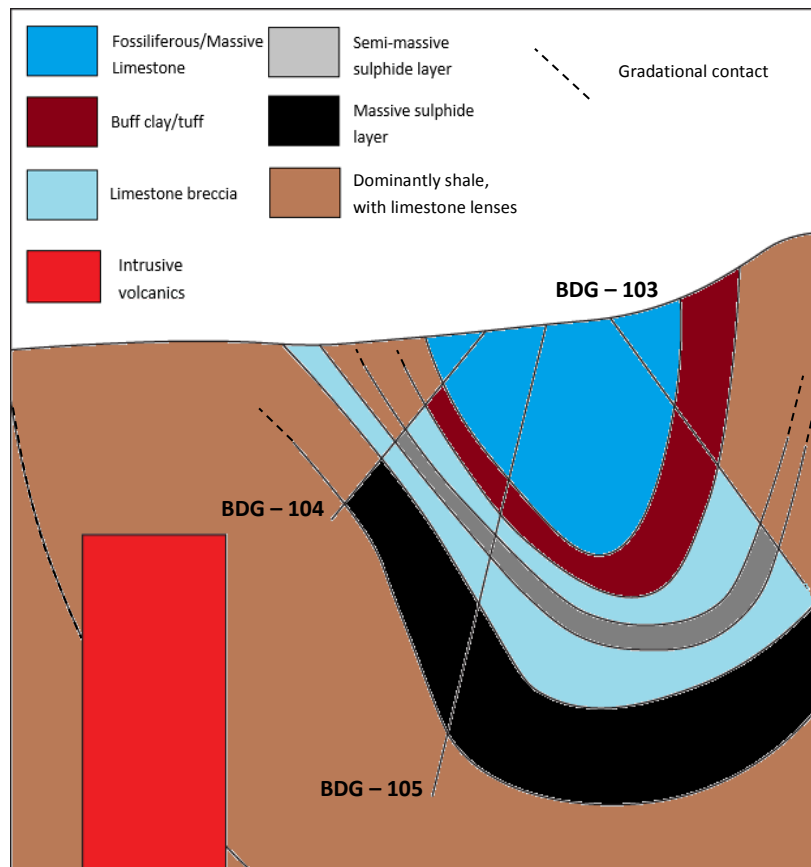
(Figure 26. Simplified cross-section representing the interpreted geological structure of the Gurubang deposit.)

Rosebank deposit area

The high-resolution magnetic and gravity data is effective in outlining specific aspects of the geological framework across the Rosebank deposit site (Figure 25 a and b). The magnetic data (Figure 25 a) clearly identifies several magnetic anomalies of varying size and shape. The elongate anomalies appear to be striking approximately N - S, which conforms to the strike identified in the regional geological interpretation by Nagy (1977). The black graphitic shale (Rabone, 1978) was identified in the eastern section of the deposit area via the magnetics survey (Figure 25 b). The unit strikes between $340^o – 350^o$ NNW-SSE and extends for the length of the survey area (strike extent confined to survey area due to limited data).

The negative gravity anomaly in the east is attributed to the major Numeralla thrust fault. Rui et. al. (1985) suggests that a fault structure can be associated with a low gravity response, potentially representing a wedge of fault gouge between the two moving plates. Also, large-scale removal of fault zone material via hydrothermal alteration, fluid transport or dissolution, may have occurred to produce this pronounce density deficiency.

5.4 GEOPHYSICAL METHODS IN SMALL-SCALE BASE METAL EXPLORATION

Ground-based TDEM survey

The result of the TDEM survey proved to be most effective at delineating the proposed sulphide mineral horizon for both target deposit areas. The technique is sensitive to the conductive mineralisation, as well as the dip of the conductive layers. This provides valuable information regarding the structural habit of the deposit. Unfortunately, each dataset was contaminated by signal noise potentially related to the presence of electric fences, atmospheric sferics or superparamagnetic rock material. Superparamagnetic iron oxide material may have weathered from exposed ferruginous gossan outcrop (present in both areas) and may be the prime cause of the EM noise. For relatively shallow deposits (50 – 100 m depth) 100 x 100 m coincident loop TDEM surveys are effective in obtaining high resolution data. Such high-resolution data can provide constraints on azimuth, dip and strike length of a target deposit. Noise contamination was reduced using multiple bin stacks and replacing the coincident loop with an in-loop setup.

Ground-based magnetic survey

The high-resolution, ground-based magnetic data obtained across the deposit areas, identifies different geological units of contrasting magnetic intensities. In terms of directly targeting the mineralisation, it would be deemed useful, assuming there are magnetic minerals (such as pyrrhotite, magnetite and/or maghemite) present within the deposit. However, as discovered when collating the data for the Gurubang site, other magnetic features can overprint the magnetic response of the mineralisation (seen by the presence of the intrusive volcanic pipe). This suggests that high resolution magnetics would be most useful in targeting and evaluating small-scale deposits that are not associated with external, highly magnetised structures.

Ground-based gravity survey

The high-resolution, ground-based gravity data were effective in outlining areas of contrasting densities associated with the overall geological framework of a target area. This study showed that the dominant geological units are the major contributors to the overall gravity response. Delineating the response associated with the small-scale deposits from the background geology proved to be difficult. The reason for not identifying the response of the mineralisation is most likely due to its small size. It is surmised that a gravity survey conducted using a tighter station spacing (~ 2.5 m intervals) may be more effective in identifying and evaluating the small-scale mineralisation.

5.5 OPTIMIZATION OF METHOD RESOLUTION

The 100 x 100 m coincident loop TDEM survey was sufficient in delineating mineralisation in both survey areas. However, replacing the coincident loop with an in-loop setup may reduce the level of noise, thus increasing the accuracy of the acquired data. As stated previously, an in-loop TDEM setup was to be tested on the Gurubang ,site, but the equipment was faulty, and the survey was not undertaken. During the Gurubang TDEM survey, a 200 x 200 m coincident loop size was trialled to compare the resolution to the 100 x 100 m loop survey. The results of the 200 m loop did not identify the presence of the mineralised horizon.

The high-resolution magnetic and gravity surveys effectively outline a variety of contrasting domains, including the mineralised horizons and geological framework of the target deposits. However, surveys at this scale are time consuming and costly for exploration companies. Therefore, the 5 m high-resolution magnetic station spacing data was compared to a synthetic dataset whereby every second station (10 m) was removed (Figure 27 a and b). The aim was to compare the resulting resolution and determine whether a wider station spacing is just as reliable in delineating and evaluating small-scale deposits. Results indicate that there is little difference in resolution between the 5 m station spacing and the 10 m spacing (Figure 27 b). Also, a similar resolution result was achieved when comparing the data to a 20 m station spacing survey (Figure 27 c). Therefore, surveys at 10 – 20 m spacing would suffice in examining these small-scale base metal deposits.

As noted previously, a portion of the high-resolution magnetic data was collected using a caesium vapour magnetometer. The caesium magnetometer provided useful data with a similar resolution to the proton. However, due to vegetation coverage the instrument was not easily utilised, and the proton magnetometer was the preferred method. This suggests that although the caesium is less robust, in the situation where there is little vegetation coverage a caesium survey at a 10 m line spacing, would give adequate detailed data.
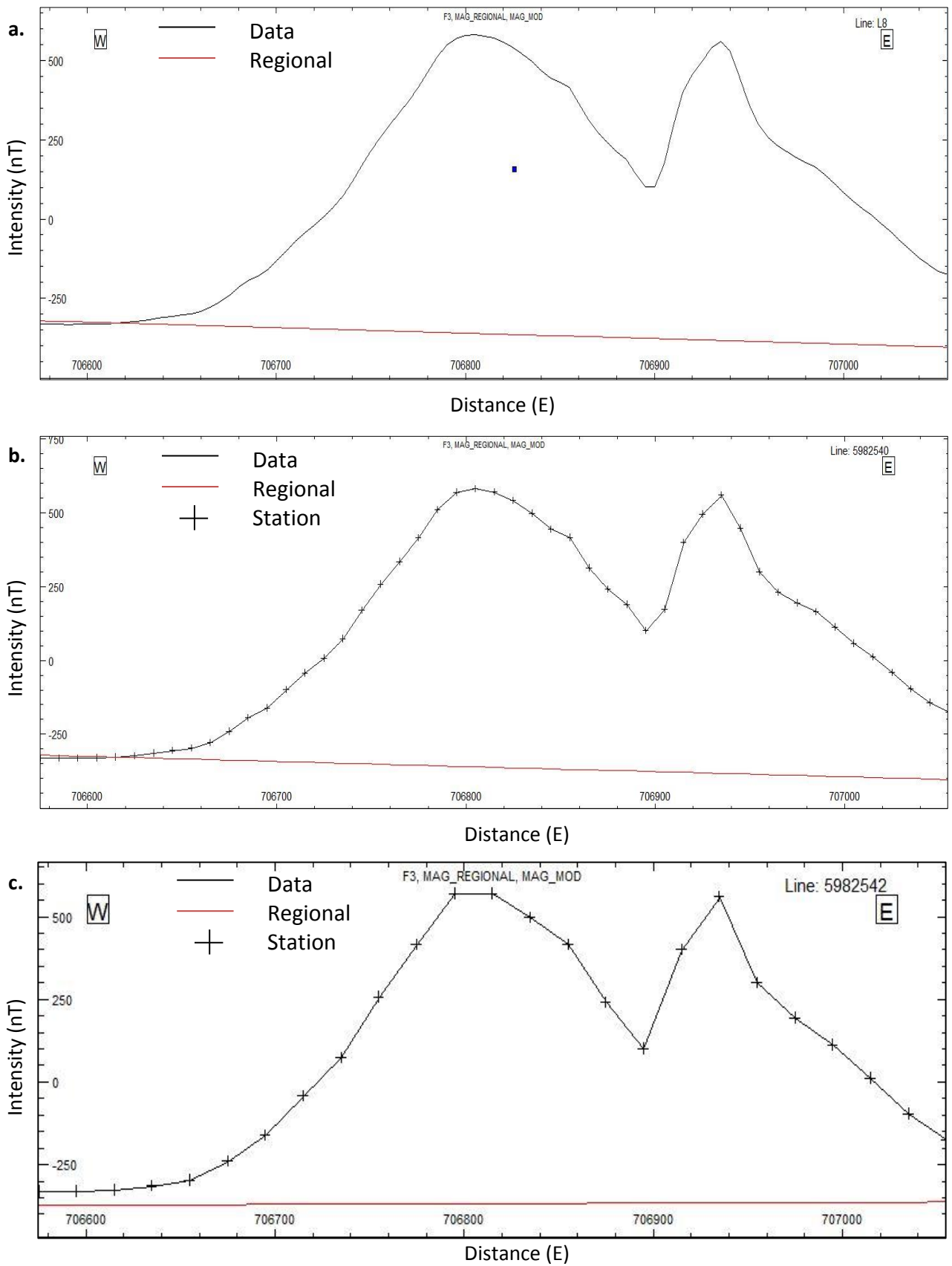
(**Figure 27. a. Gurubang magnetic anomaly response using 5 m station spacing.
b. Gurubang magnetic anomaly response using 10 m station spacing.
c. Gurubang magnetic anomaly response using 20 m station spacing.**)

CHAPTER 6

CONCLUSION

This study aimed to assess the effectiveness of various high-resolution geophysical techniques in delineating two small-scale base metal deposits in south eastern NSW. In making this assessment the study also characterised the local geological framework via the detail geophysical data. From this information, the following conclusions were made:

1. The 100 x 100 m coincident loop TDEM survey was effective in delineating and evaluating the small-scale base metal deposits. The technique was sensitive to the conductive mineralisation abundant in each deposit setting. It was also effective in evaluating the apparent dip of the mineralised layers.

   - The Gurubang TDEM survey successfully outlined two conductive horizons; a shallow horizon extending to a depth ranging from $100 - 150$ m and a deep horizon extending to a depth of $200 - 250$ m. The method was useful in constraining the dip of the horizons ($45^o - 70^o$). It confirmed that the deposit occurs in an open to close synclinal formation and that the mineralisation trends NNW – SSE extending for the length of the survey area.

   - The Rosebank TDEM data successfully showed that the mineralisation occurs in a single relatively thin lens, with an apparent dip ranging from $50^o - 60^o$ towards the west. TDEM modelling showed a strike length of approximately 100 m. The survey was also effective in identifying the previously discovered black 'graphitic' shale unit and constrained the dip of the shale unit to 50° towards the west.

2. The 5 m spacing, high resolution magnetic survey is sufficient for delineating areas of sulphide mineralisation. However, as seen in the case of the Gurubang deposit, the method is less effective when other unknown structures contribute to the total magnetic signature. The 5 m spacing gravity method may be useful in identifying the small-scale mineralisation, but this depends on the density contrast between the orebody and the host stratigraphy.

3. The 5 m spacing, high-resolution magnetic and gravity surveys effectively outline the geological framework, as well as some previously unidentified structures, comprising both target areas.

   - The magnetic and gravity survey effectively identified features such as, a large intrusive basaltic pipe/plug and major and minor faults (Numeralla Fault) and folds.

   - The magnetic and gravity surveys also identified the general (NNW – SSE) trend of the basement geology in the both deposit areas.

- The magnetic method successfully constrained the dip, strike length and thickness of the black shale unit in the Rosebank deposit area.
- It also successfully identified the Tertiary basaltic cover unit.

4. Undertaking a 10 – 20 m spaced, ground-based magnetic and gravity survey would obtain a similar data resolution to the run 5 m spacing surveys. It is assessed that a line spacing of 20 m would suffice in delineating the small-scale deposits.

5. The cesium magnetometer provided adequate high-resolution magnetic data, but the method is less robust in vegetated terrain. If the terrain suits a proton magnetometer then a 10 m spaced survey would suffice and provide data with enough detail to evaluate the target small-scale mineralisation.

REFERENCES

Airo, M-L., (2015). Geophysical Signatures of Mineral Deposit Types – Synopsis. *Geophysical signatures of mineral deposit types in Finland*. Geological Survey of Finland, Special Paper 58, 9–70, 2015

Argaud, M. J., (1976). Geophysical Interpretation at Gurubang, NSW. *Aquitaine Australia Minerals*. Report No. MG: 690

Castle M. J., (1976). Summary Report on Diamond Drilling Programme at Gurubang Prospect: EL 786 Dangelong (Cooma), NSW. *Aquitaine Australia Minerals*. Report No. MG 712

Cooke. J., (1977). EL 786 Dangelong: Gurubang Mapping Project. *Aquitaine Australia Minerals*, Report No. MG 797

Dentith, M., & Mudge, Stephen T., (2014). *Geophysics for the mineral exploration geoscientist.* Cambridge Cambridge University Press. 2014.

Elliot, J. D., (1983). Third Annual Report to End January. *Australian Occidental Pty. Ltd*., Minerals Division

Ford, K., Keasting, P. and Thomas, M. D., (2007). Overview of geophysical signatures associated with Canadian ore deposits. *Geological Association of Canada*, Mineral Deposits Division, Special Publication, no.5, pp.939-970.

Foster, D., & Gray, D., (2000). Evolution and Structure of the Lachlan Fold Belt (Orogen) of Eastern Australia. *Annual Review of Earth and Planetary Sciences*, 28(1), 47-80.

Galley, A. G., Hannington, M., and Jonasson, I. R., (2007), Volcanogenic massive sulphide deposits, in Goodfellow, W. D., ed., Mineral Deposits of Canada: A Synthesis of Major Deposit-Types, District Metallogeny, the Evolution of Geological Provinces, and Exploration Methods: Ottawa, Canada, *Geological Association of Canada,* Mineral Deposits Division, p. 141-161.

Gemmell, J. B., Large, R. R. and Zaw, K., (1998). Palaeozoic volcanic-hosted massive sulphide deposits. *AGSO Journal of Australian Geology and Geophysics*, 17(4), 129 – 137

Gray, D., (1997). Tectonics of the southeastern Australian Lachlan Fold Belt: Structural and thermal aspects. *Geological Society, London, Special Publications*, 121(1), 149-177.

Gibson, H. L., Allen, R. L., Riverin, G., and Lane, T. E., (2007), The VMS model: advances and application to exploration targeting, in B. Milkereit, ed., *Proceedings of Exploration 07: Fifth Decennial International Conference on Mineral Exploration*, 713–730.

Gunn, P. J. and Dentith, M. C., (1997). Magnetic responses of mineral deposits. *AGSO Journal of Australian Geology & Geophysics*, 17(2), 145 – 158

Herzberger, G. A., Barnes, R. G. and Bowman, H. N., (1976). A metallogenic study of the Bega 1:250,000 sheet SJ55-4. *Geological Survey of New South Wales*, Sydney.

Horsburgh. J., (1983). Annual Report for Period Ending 8th February. *Getty Oil Development Company, Ltd*.

Lewis P.C., Glen R.A., Pratt G.W. & Clarke I., (1994). Bega-Mallacoota 1:250 000 Geological Sheet SJ/55-4, SJ/55-8 Explanatory Notes, 148 pp, 8 pls. *Geological Survey of New South Wales*, Sydney.

McQueen, K. G., (1994). The Tertiary Geology and Geomorphology of the Monaro: The Perspective in 1994. *Centre for Australian Regolith Studies*. Occasional Publication No. 2

Morgan, L.A., and Schulz, K.J., (2012), Physical volcanology of volcanogenic massive sulfide deposits in volcanogenic massive sulfide occurrence model: *U.S. Geological Survey Scientific Investigations* Report 2010–5070–C, chap.6, 8p

Nagy, L. J., (1977), EL 898 Skidmore, NSW: for 6 months ending August. *Report for Abminco N. L.* (GS1977/027)

Scott, Ashley, & Lawie., (2001). The geochemistry, mineralogy and maturity of gossans derived from volcanogenic Zn–Pb–Cu deposits of the eastern Lachlan Fold Belt, NSW, Australia. *Journal of Geochemical Exploration*, 72(3), 169-191.

Slack, J.F., Foose, M.P., Flohr, M.J.K., Scully, M.V., and Belkin, H.E., (2003). Exhalative and subsea-floor replacement processes in the formation of the Bald Mountain massive sulfide deposit, northern Maine, in Goodfellow, W.D., McCutcheon, S.R., and Peter, J.M., eds, Massive sulfide deposits of the Bathurst mining camp, New Brunswick, and northern Maine: *Society of Economic Geologists*, Economic Geology Monograph 11, p. 513-547.

Smith Engineering Systems., (2015). Annual Report Exploration License Number 6940. *Report to the NSW Geological Survey*. December 2015

Wang, C., Rui, F., Zhengsheng, Y., & Xingjue, S., (1986). Gravity anomaly and density structure of the San Andreas fault zone. *Pure and Applied Geophysics, 124*(1), 127-140.

Wilson, M. J., (1994). Annual Report for Exploration License Number 4605. *Report for Denehurst Limited.* October 1994.

SUPPLEMENTARY MATERIAL

There is no supplementary material for this thesis.